# Energy Walls

by

**Maria Canellas (HO)**

**Fourth-year Undergraduate Project**

**in Group D, 2011/2012**

**Supervisor: Prof. Kenichi Soga**

*I hereby declare that, except where specifically indicated, the work submitted herein is my own original work.*

# Energy Walls

## 1.0 Introduction

Two major challenges faced by modern society are energy security, and lowering carbon dioxide gas emissions. Energy walls have a large potential to aid in the remediation of these problems, since they are a sustainable energy-providing technology that uses soil as a heat exchange medium. However, extensive research is required to determine the effects of cyclic heating and cooling on their geotechnical and structural performance.

## 2.0 Main Research Objectives

The energy walls project is based on the Crossrail Dean Street station energy wall, which is designed to provide 200kW-1MW of energy for station space and water heating only. The main aim of the project is to build a Finite Element (FE) model of the station, and analyse the complex thermo-hydro-mechanical behaviour of the structure.

## 3.0 Experimental Procedure

A 2D representative section of the Dean street station is modelled as a finite element mesh, using Hypermesh software. The analysis is performed using LS-DYNA software, which has the ability to couple soil mechanics, thermal and fluid mechanics analyses, for multi-phase media such as soils. The thermal operation of the energy wall is modelled as consecutive 6-month cycles of cooling and recharge, as summarised in Figure 1.

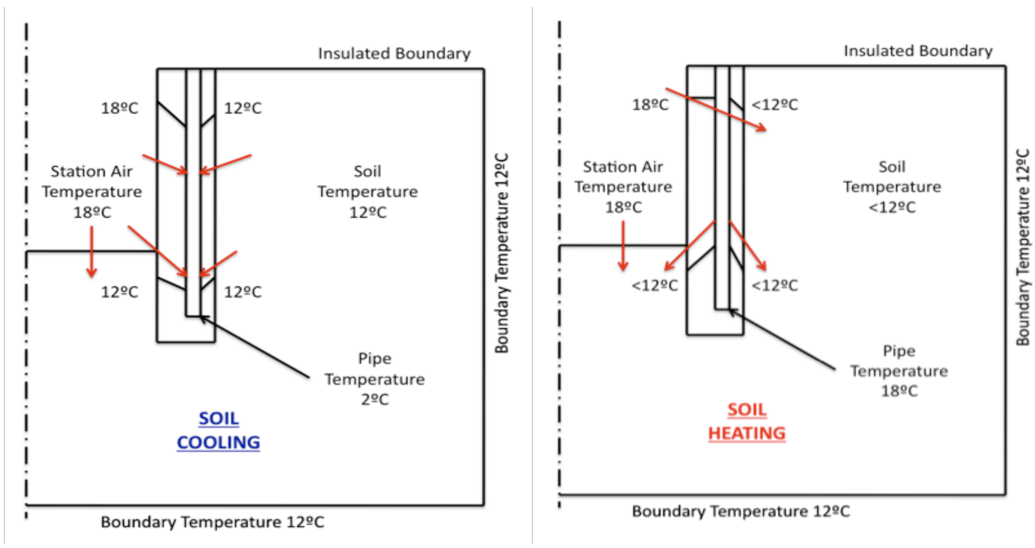


**Figure 1 – Energy wall seasonal operation**

Red arrows show heat flow direction, down the temperature gradients.

## 4.0 Results and Discussion

The thermal operation of the energy wall influences the geotechnical performance of the soil and the structural performance of the diaphragm wall. During cooling operation, the soil skeleton shrinks due to thermal contraction, which decreases the total stress in the soil. Due to cooling, the pore fluid is subjected to contraction, thus reducing the pore pressure in the soil. As a result, the displacement of the diaphragm wall decreases, and soil surface settlement increases due to soil matrix contraction. As pore pressure is allowed to drain out of the pores, further settlement and displacement changes are induced. During soil heat recharge, the temperatures within the soil and energy wall increase. Therefore, the reverse trends to cooling are observed in heating. Stress redistributions due to thermal cycles cause the bending moment on the diaphragm wall to increase (as shown in Fig.2). Given that the GSHP pipe is installed within the diaphragm wall, differential thermal strains are induced across the width of the wall, which induce additional bending moments on the wall.

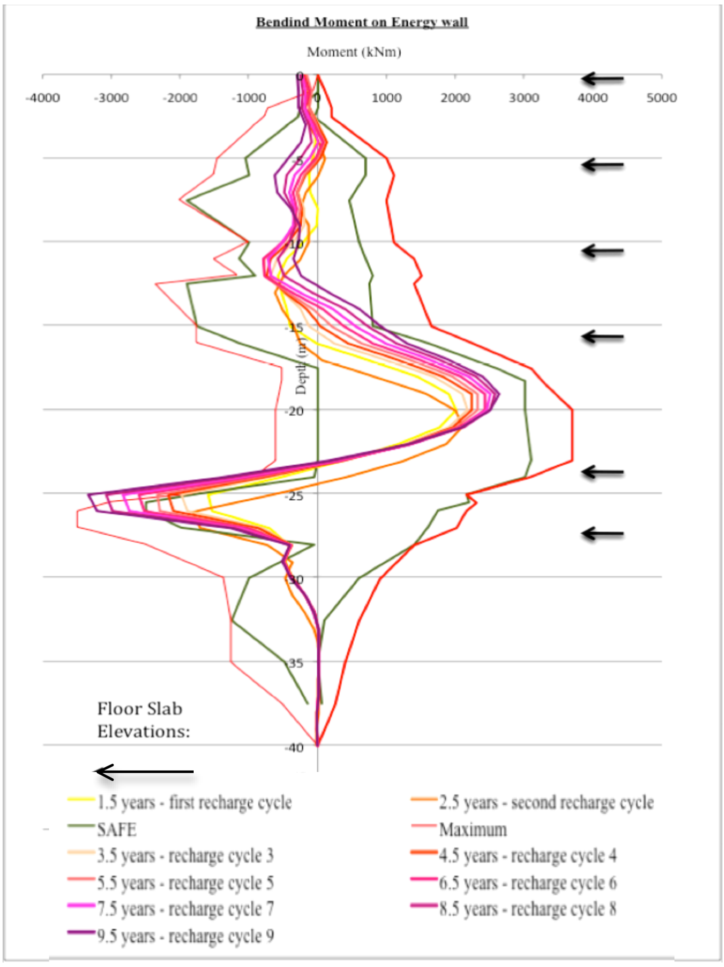


**Figure 2 – Bending moment on energy wall due to thermal operation**

## 5.0 Conclusion

The cyclic thermal operation of the energy wall affects its geotechnical performance. The main concern raised by this analysis is the magnification of displacement, settlement and bending moment changes with consecutive thermal cycles. It is thought that the cyclic thermal operation of the energy wall will cause soil strength degradation, which could compromise the stability of the diaphragm wall. For this reason, further investigation of the thermo-hydro-mechanical behaviour of energy walls is required, in order to evaluate their long-term stability and confirm their safety for continued use.

**“Energy Walls”**
**Final Report**

**Index**

**List of Figures**

**List of Tables**

## 1.0 Introduction

Two of the major challenges faced by modern society are the depletion of finite energy resources and increased carbon dioxide gas concentrations in the Earth's atmosphere. Both factors are highly interlinked with the greenhouse effect and climate change, which are further exacerbated by rapid population growth and increasing living standards. Given the international repercussion of the aforementioned topics, remedial actions and solutions have been sought worldwide, over the last 20 years. However, it was with the approval of the Kyoto Protocol in 1997, that these issues gained most relevance. At this point, the development of technologies to exploit renewable energy resources became imperative, as a step towards the replacement of finite with sustainable energy resources.

Building space and water heating and cooling, account for almost a sixth of the total global energy consumption (International Energy Agency, 2011). Therefore, the development of renewable energy technologies is vital, in order to relieve the pressure on finite fossil fuels, preserve the environment, and reduce carbon dioxide emissions. One of such technologies is a Ground Source Heat Pump (GSHP), which has lead to the creation of energy foundations and energy walls.

### 1.1 Literature Review

#### 1.1.1 Ground Source Heat Pumps (GSHPs)

Ground Source Heat Pumps (GSHPs) have become an increasingly popular technology for the provision of sustainable heating and cooling energy for housing, offices and retail spaces. Their operation relies on the temperature differences between atmosphere and soil at depths greater than 10m (Fig. 1.1). At such depths, the temperature of the soil remains constant at around 10ºC (in Europe), which means there is a year-round temperature difference between soil and atmospheric air. Therefore in winter, the excess heat in the soil (compared to the air) can be extracted for space heating, and in summer, excess heat in the air can be transferred into the soil as a means of space cooling. This balanced operation allows soil heat recharge, ensuring the soil is never too cold to hinder future operation of the GSHP.

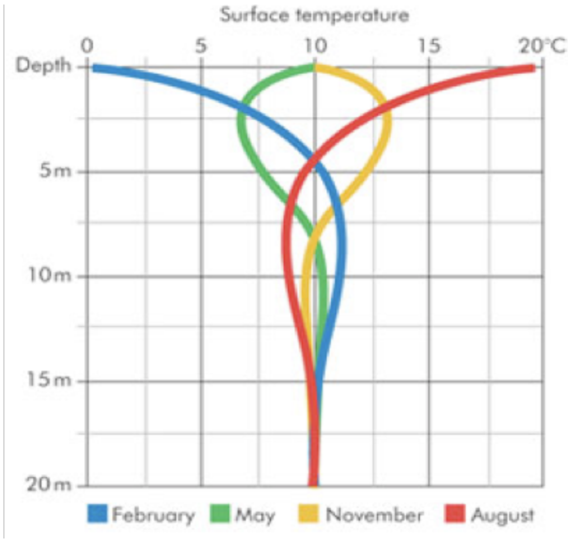


**Figure 1.1 - Annual temperature fluctuations of surface soil with depth.** **(FWT Ltd., Bibliography [28])**

The main components of a GSHP (Fig 1.2) are an underground primary circuit, a secondary circuit for a heat-distribution system, and a heat pump. The heat pump uses a small fraction of electrical energy to convert the low temperature heat from the soil, to higher temperature heat for space and water heating.

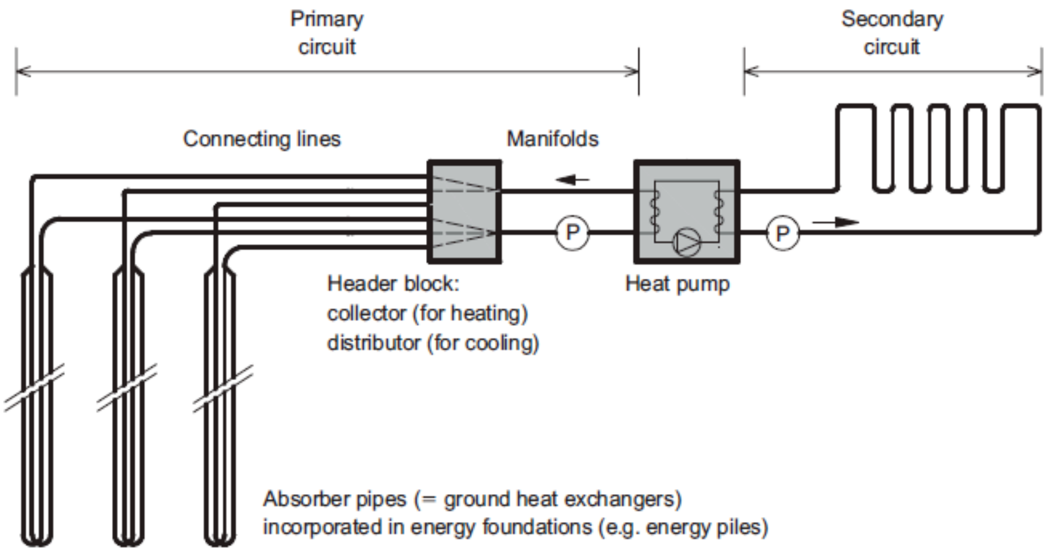


**Figure 1.2 - Ground Source Heat Pump components.** **(H.Brandl, (2006)) Bibliography [1])**

Such systems have been implemented since the 1970s, and "as of 2004 over one million units have been installed worldwide" (The Green Age). While it is true that GSHPs suppose a high initial investment cost, they offer numerous benefits to their immediate users and surroundings. GSHPs offer a reduction in fuel costs, as well as being more aesthetically pleasing, less noisy, and requiring less maintenance than conventional heating and cooling systems. Furthermore, GSHPs require no fuel transportation or storage at the site, and they can reduce energy consumption by as much as 50% compared to direct electric heating, thus reducing $CO_2$ emissions significantly.

### 1.1.2 Energy Foundations

Since their technology is well established and proven, the primary circuits of GSHPs have been installed into concrete foundation elements to form thermo-active foundations, making use of the high thermal storage capacity of concrete. This is a sustainable practice since it makes use of foundations as dual-purpose structures: load-bearing and energy-providing. The first examples of such systems date to the 1980s, with the first energy piles and walls being installed in Austria and Switzerland in 1984 and 1996 respectively (H.Brandl, 2006). Thermo-active foundations have gained popularity within the UK over the last 10 years, with energy piles being installed in Keble College (Oxford 2001), Paddington Building (London 2007) and Lambeth College (London 2007). The first energy wall in the UK was installed at the Bulgari Hotel in London in 2010 (Fig. 1.3), triggering a boost in the implementation of such systems in other high-profile projects such as Crossrail.

**Figure 1.3 – Primary circuit of the energy wall at the Bulgari Hotel.** **(Geothermal International Ltd.(2010)) Bibliography [12])**

## 1.2 Outstanding Issues

Since the first implementation of GSHPs, numerous investigations and research projects have been undertaken to assess several aspects of the technology. Research has been performed to assess and improve the efficiency and viability of GSHPs. Furthermore, extensive research has been performed to improve measurement methods for the mechanical and thermal properties of soil, in an attempt to improve GSHP design.

In terms of thermo-active foundations, several investigations have been performed to assess the economic and technical viability of using different underground structures, such as underground tunnels, as sources of energy. In-situ tests have been performed to investigate the "geotechnical and thermodynamic aspects of pile response to heat cycles" (P.J.Bourne et al, 2009), which have served to develop and calibrate analytical models, to investigate the behaviour of energy piles.

Computational methods have been developed to analyse the thermal response of energy walls. However, very limited information is available concerning the thermo-mechanical response of energy walls to heating and cooling cycles. It is known that the energy wall and surrounding soil will expand and contract, due to thermal stresses. However, the impact of these effects is still unknown. It is therefore important that both computational and in-situ tests are performed on energy walls, to analyse the effects of heating and cooling cycles on their short and long-term geotechnical performance.

### 1.3 Main Project Objectives

Crossrail is a major rail project in London, which intends to reduce train journey times by allowing trains to cross the city through an underground rail network. The project started in 2008 and is due for completion in 2018. The project team decided to incorporate energy foundations in 6 stations including Liverpool Street, Paddington, and Tottenham Court Road at Dean Street. This design decision has the potential to save 350 tonnes of $CO_2$ per annum, by including numerous energy piles and energy walls within the stations.

The Energy Walls project is based on the Dean Street station energy wall, which has already been constructed, and will be used to provide 200kW-1MW of energy for station space and water heating only. Arup, who have performed preliminary thermal analyses for the GSHP system, designs the station. The main aims[1] of the project are:

- Building a coupled thermo-mechanical Finite Element (FE) model of the Dean Street station.
- Analysing the complex thermo-hydro- mechanical interactions between soil and structure, to evaluate the structural response of the diaphragm wall to heating and

[1] Project Programme Included in Appendix A.2.

cooling cycles. The bending moments and displacements of the Energy Wall will be analysed using FE analysis, to ensure the bending moments induced on the wall do not surpass its plastic moment capacity.

## 2.0 Project Design

Soil is a multi-phase medium (soil particles, air and water), therefore requiring a more complex analysis compared to a single-phase medium. When performing coupled thermo-hydro-mechanical analyses, the complex mechanisms involved increase, requiring specialised FE software to produce a realistic analysis. Oasys LS-DYNA is selected for the analysis, given its capability to model pore fluid, as well as soil skeleton, thermal expansion. Furthermore, LS-DYNA is the preferred software tool used by Arup to perform their analyses of the energy wall, and therefore results from both analyses can be compared to assess the validity of the Energy Walls project results[2].

### 2.1 Theoretical Basis

LS-DYNA is a "multi-purpose explicit and implicit finite element programme" (Oasys Ltd.), which has the ability to analyse soil mechanics, thermal and fluid mechanics problems, for multi-phase media such as soils. The analyses can be performed as stand-alone or they can be coupled to represent reality more closely.

#### 2.1.1 Governing Equations for Analysis

LS-DYNA relies on mass, momentum and energy conservation.

Mass Continuity

$$\partial\rho/\partial t + \nabla \cdot (\rho \mathbf{v}) = 0$$

Momentum Conservation

$$\partial(\rho \mathbf{v})/\partial t + \nabla \cdot (\rho \mathbf{v}^2) = \nabla \cdot \boldsymbol{\sigma} + \rho \mathbf{g}$$

Energy Conservation (for each single-phase material)

$$\partial(\rho c_p T)/\partial t + \nabla \cdot (\rho c_p T \mathbf{v}) = \nabla \cdot k\nabla T + H$$

[2] The version of LS-DYNA used is not commercially available. Instead, it has been modified by Arup to model, for example, pore fluid thermal expansion.

Where, $\rho$ is the density, $\mathbf{v}$ is the vector for velocity, t is time, $\mathbf{g}$ is the vector term for acceleration due to gravity, $\boldsymbol{\sigma}$ is the stress tensor in the material, k is the thermal conductivity, T is the temperature, $c_p$ is the specific heat at constant pressure, and H represents the heat input from all sources.

Soil Characterisation

The soil is characterised by a constitutive model that expresses stresses as a function of strains.[3] The soil is assumed to follow Terzaghi's principle of effective stresses, whereby the effective stress on the soil is the total stress minus the pore pressure.

Pore Fluid Characterisation

The pore fluid is incompressible, and assumed to follow Darcy's Law:

$$q_h = -k_h \nabla H$$

Where $q_h$ is the flux (flow per unit area), $k_h$ is the permeability of the soil, and $\nabla H$ is the vector form of the hydraulic gradient driving the fluid.

Heat Transfer Mechanisms

Heat transfer mechanisms in soil are complex due to its multi-phase nature and include conduction, convection, radiation vaporisation and condensation, ion exchange and freeze-thawing processes (H.Brandl, 2006). However, for the energy walls project only conduction and convection are modelled, since their contribution is largest. Since pore fluid velocity is small at all times, convective heat transfer is small, and therefore conduction dominates. Heat conduction is assumed to follow Fourier's Law:

$$q_T = - k_T \nabla T$$

Where $q_T$ is the heat flux, $k_T$ is the thermal conductivity and $\nabla T$ is the vector form of the thermal gradient driving the fluid.

[3] Constitutive model selected is Mohr-Coulomb. Further information in section 3.0.

Volumetric Stains on Soil and Pore Fluid

Assuming compression is positive, the volumetric strain on the soil skeleton is computed as a function of 3 terms, as shown below. The first contribution is due to stress changes on the soil skeleton in 3 dimensions. The second term represents the soil skeletal expansion due to soil grain expansion. The final term is due to soil skeleton shrinkage due to structure collapse.

$$\varepsilon_{v(skeleton)} = tr[D^{-1}(d\sigma - dp)] - \alpha_{s-g}dT + \alpha_{s-s}dT$$

Where T is the temperature, $\alpha_{s-g}$ is the thermal expansion coefficient of the soil grains, $\alpha_{s-s}$ is the thermal contraction coefficient due to structure collapse, σ is the stress in the soil, p is the pore pressure, D is the stiffness matrix, and "tr" indicates that the volumetric strain in 3 dimensions is calculated as a function of varying effective stresses and pore pressures.

Given that pressure and temperature changes, as well as drainage conditions affect the pore pressure, pore fluid is subjected to volumetric strains. In this case, the volumetric strain is a function of thermal expansion of the fluid, volumetric compression due to pressure increases, and water flow out of the pores:

$$\varepsilon_{v(porewater)} = -n\alpha_w dT + (n/K_w)dp + q_w$$

Where T is the temperature, n is the porosity, $\alpha_w$ is the thermal expansion coefficient of pore water, $K_w$ is the bulk modulus of pore water, p is the pore pressure and $q_w$ is the pore water flux (flow of pore water out of the pores per unit area). If the conditions are undrained, $q_w = 0$.

In order to satisfy the kinematic conditions of volume conservation, both volumetric strains must be equal and therefore the following equations apply:

$$tr[D^{-1}(d\sigma - dp)] - \alpha_{s-g}dT + \alpha_{s-s}dT = -n\alpha_w dT + (n/K_w)dp + q_w$$

$$tr[D^{-1}(d\sigma - dp)] + (n/K_w)dp + (n\alpha_w - \alpha_{s-g} + \alpha_{s-s})dT = q_w$$

Fully coupled Thermo-Hydro-Mechanical Model

The analysis performed in LS-DYNA is a coupled thermo-hydro-mechanical analysis, which unites all the theory and equations mentioned previously, to solve the coupled system of equations (Y.Rui, 2011):

$$\begin{cases} \partial^T [D]\left([\partial]\{d\delta\} - \{d\varepsilon\}^H\right) - \nabla dp = 0 \\ \nabla^T [k] \nabla p + \frac{\partial}{\partial t}\nabla^T \{\delta\} + \frac{1}{k_w}\frac{\partial p}{\partial t} + (\alpha_s - n\alpha_w)\frac{\partial}{\partial t} T = 0 \\ \rho_w c_p \frac{\partial}{\partial t} T - \nabla^T D \nabla T + c_p^w k_h \nabla^T (T \nabla p) = 0 = 0 \end{cases}$$

Where $\{d\varepsilon\}^H = \alpha\begin{bmatrix}1 & 1 & 1 & 0 & 0 & 0\end{bmatrix}^T dT$ and δ is the displacement. All the other variables are defined as in previous equations. The system of coupled equations is solved explicitly by LS-DYNA.

### 2.1.2 FE Numerical Integration Techniques

For this specific problem, given the displacements of soil are small, the analysis is quasi-static, and is performed using Gauss Point numerical integration. The LS-DYNA quasi-static analysis is done by performing regular numerical integrations, with independent thermal and structural analysis timesteps. The analyses are then coupled by treating displacement, pore pressure and temperature fields as constants for the thermal, hydraulic and mechanical analyses.

## 2.2 Difficulties with LS-DYNA

LS-DYNA software has the capability to solve highly complex problems and therefore presents benefits other software packages cannot offer. However, the LS-DYNA user interface is poor, which makes the software hard to manipulate. A text file containing all analysis parameters must be written for every analysis, and each parameter is displayed as a single number, with no indication of its meaning or units. Furthermore, the format of the text file is very specific, with a designated number of spaces between each parameter entry. As shown on the next page, on the second line of the code, the third entry from the left (bold characters) is the elastic shear modulus of made ground and it reads as 10000, meaning 10MPa. If an extra space is introduced between the second and the third entry, the elastic shear modulus is read as 1000. This value is an order of magnitude smaller than it should be, which may have a drastic impact on the analysis results.

………1…….1.8..…**10000**……0.25………0…..0.436…….0.0…….0.0

This high specificity facilitates the introduction of mistakes into the code, which may stop the analysis from running, or may result in incorrect results. Furthermore, these errors can only be detected by visual checks, which are time-consuming and inaccurate. In addition to these difficulties, the version of LS-DYNA used is not commercially available, and instead has been created by Arup, who have changed the LS-DYNA source code to introduce modelling capabilities such as pore fluid thermal expansion.  Therefore, there are no publically available manuals to accurately indicate what each parameter in the text file represents. The author of this report used commercially available LS-DYNA manuals to create the preliminary text files. However, since some parameter definitions had been changed, incorrect results were obtained at different stages of the analysis, thus hindering progress.

## 3.0 Dean Street Analysis

Dean Street station box is part of the Tottenham Court Road Crossrail Station, and is located at the intersection between Dean Street and Oxford Street (Fig. 3.1). The existing buildings at the site have been demolished, and the station is constructed by excavation with temporary supports, prior to bottom-up construction of the inner structure. Since the station is located in a highly urbanised and transited area, the settlements induced by the station construction and subsequent energy wall operation must remain within safe limits.

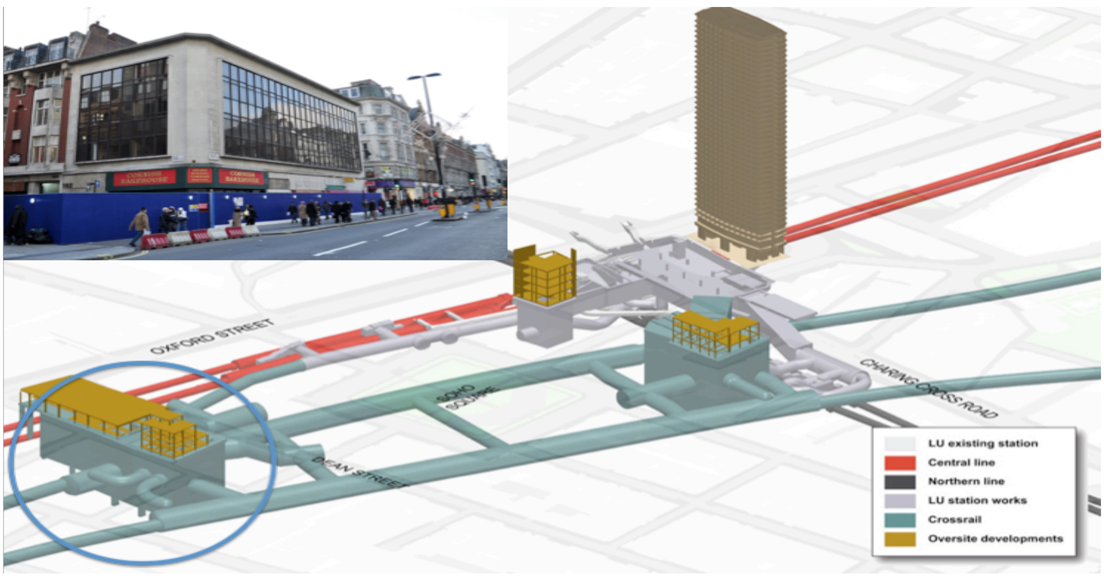


**Figure 3.1 – Dean Street station location** (Arup (2011) & Flickr, Biblio [26] & [30])

## 3.1 2D FE Model

The station is composed of two main boxes with different base levels. They comprise numerous piles, which will be used to support the station floor slabs and subsequent over-site construction. Some of these piles are energy piles, and all the perimeter diaphragm wall panels are part of the energy wall.

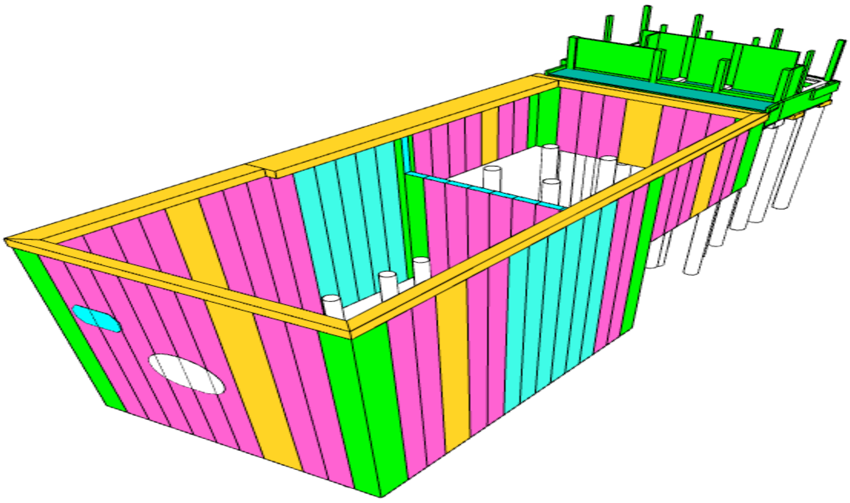

**Figure 3.2 – 3D CAD drawing of Dean Street station** (Arup (2011)).

The width of the station changes with length, which imposes difficulties when creating a realistic 2D model of the station. However, through geometrical simplification, and using Hypermesh software, a 2D representative model of the station is created. The main model dimensions are summarised in Figure 3.3.

The mesh is composed of rectangular elements, and is finer closer to the energy wall, which is where most stress concentrations, and highest temperature gradients are expected to occur. Although the model analyses a 2D problem, it has an in-plane width of 0.25m (one element). The model shows the site soil stratification, and the different concrete elements of the station. Drainage is allowed to occur at the bottom and left-hand-side boundaries of the model.

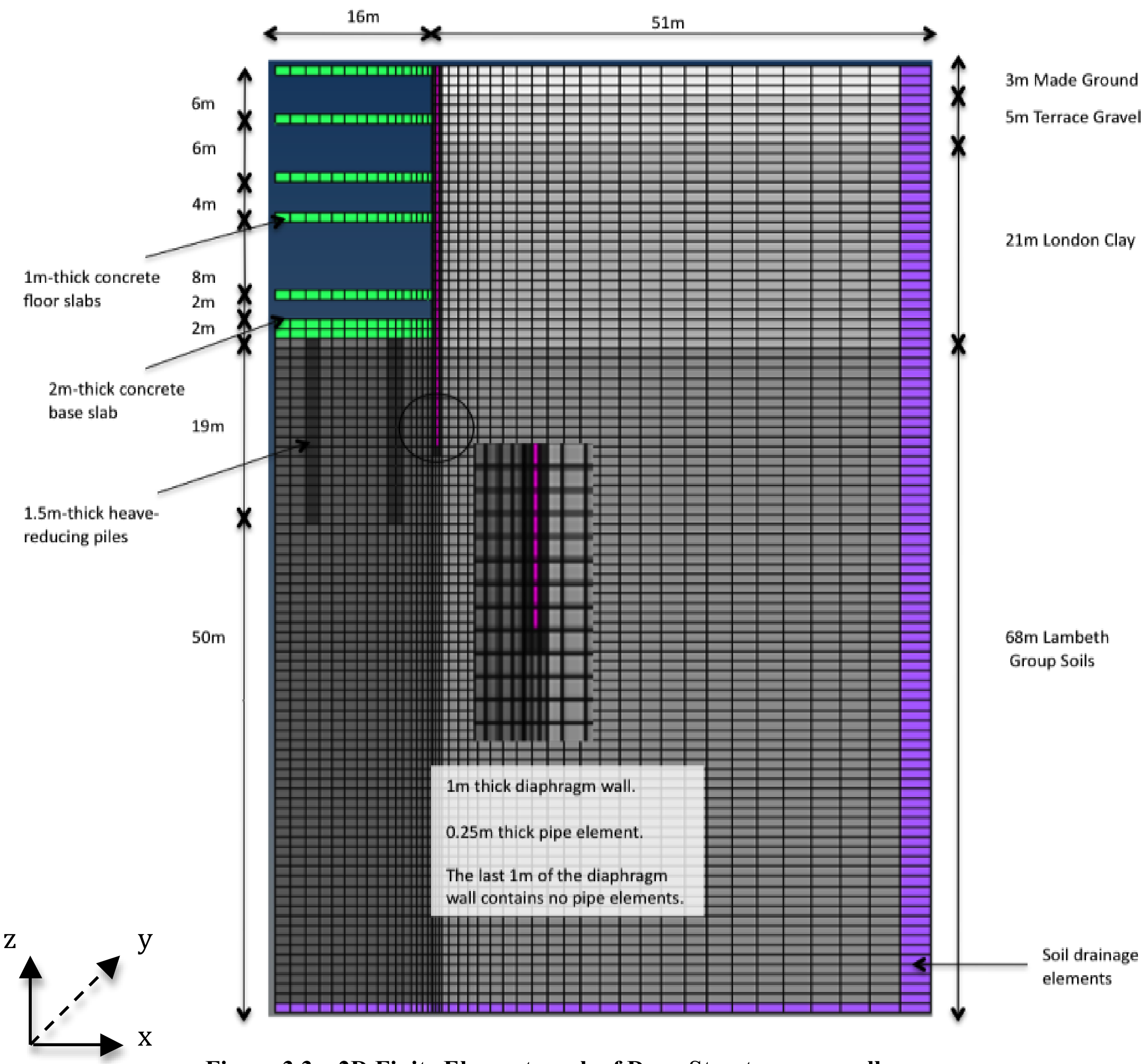


**Figure 3.3 – 2D Finite Element mesh of Dean Street energy wall.**

### 3.1.1 Boundary Conditions

Rotation and translation boundary conditions have been imposed on the model as summarised in Table 3.1. All the nodes in the model are restrained in terms of rotation and translation in the in-pane direction (y-direction), since the model is 2D and cannot represent in-plane mechanisms.

| Node Boundary | Rotation and translation | | |
|---|---|---|---|
| | x | y | z |
| Top surface of soil and wall | Free | Fixed | Free |
| Right-Hand-Side | Fixed | Fixed | Free |
| Left-Hand-Side | Fixed | Fixed | Free |
| Bottom Boundary | Fixed | Fixed | Fixed |
| All remaining nodes in the model | Free | Fixed | Free |

| Free: | (green) | Fixed: | (red) |
|---|---|---|---|

**Table 3.1 – Rotation and translation boundary conditions**

## 3.2 LS-DYNA

### 3.2.1 Analysis Procedure

The analysis of the energy wall is conducted in three consecutive stages, each of which builds on the results of the previous stage.

1. The first step of the analysis represents the construction of the station. The diaphragm wall is installed first, prior to excavation. The station box is then excavated in stages, using temporary steel props, followed by a bottom up construction of the concrete floor slabs. This stage is modelled as undrained, since it is assumed that construction will occur at a higher rate than pore pressure dissipation.

2. The following stage of the analysis models one year of time-dependant soil consolidation, with no thermal effects. One year was selected, since this is a realistic time between the end of construction and start of operation of the station. The drainage of the pore fluid occurs at the right-hand-side and bottom boundaries of the model (as indicated in Figure 3.3 – Section 3.1).

3. The third stage of the analysis models the first 9 years of energy wall operation. This stage models the thermo-hydro-mechanical behaviour of the energy wall.

### 3.2.2 Seasonal Operation of Energy Wall

The Dean Street energy wall is designed to provide space and water heating only. The station air temperature is to be kept constant at around 18ºC throughout the year, which dictates that the energy wall will be operative during only 6 months (winter season), allowing natural soil heat recharge during the following 6 months (summer season).

The temperature in the soil skeleton and pore fluid is assumed to be the same at each point in time. Initially, all station elements are at 12ºC, and therefore this is the far-field boundary temperature. For simplicity, the soil surface is treated as insulated, therefore ignoring surface recharge from solar radiation. The station box walls and floor boundaries are maintained at 18ºC constantly throughout all analyses. The pipe temperature is varied every 6 months, from 2ºC during the "winter" operation, to 18ºC during the "summer" operation, as shown in Figure 3.4. (The pipe temperature has to be set to 18ºC to simulate the inoperative state of the energy wall during summer, due to modelling limitations).

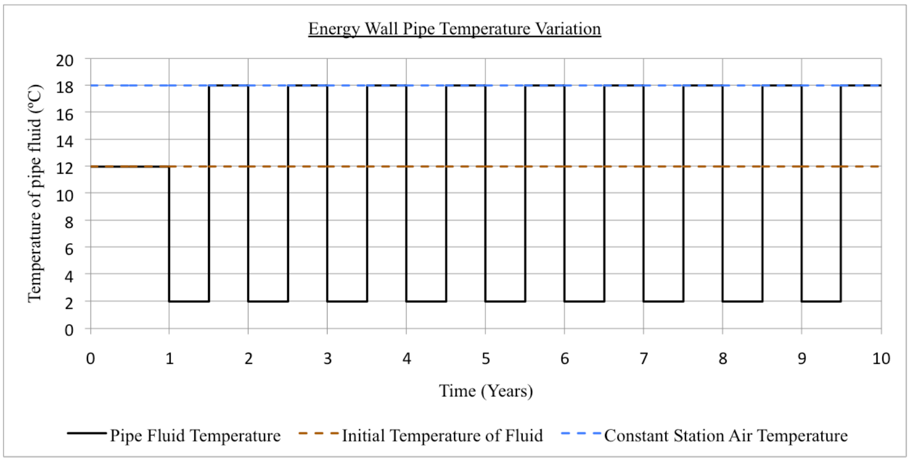


**Figure 3.4 – Energy wall pipe temperature variation throughout 10 years of operation**

The boundary conditions and heat flow direction for the seasonal thermal analysis are summarised in Figure 3.5. The initial winter operation soil temperature will be 12ºC. Given heat will be extracted from the soil in winter the initial summer operation soil temperature will be less than 12ºC. It is expected that the soil temperature for the subsequent winter operations will be greater than 12ºC. This is because the previous 6 months of heat recharge, will have allowed the 18ºC station air temperature to propagate into the soil.

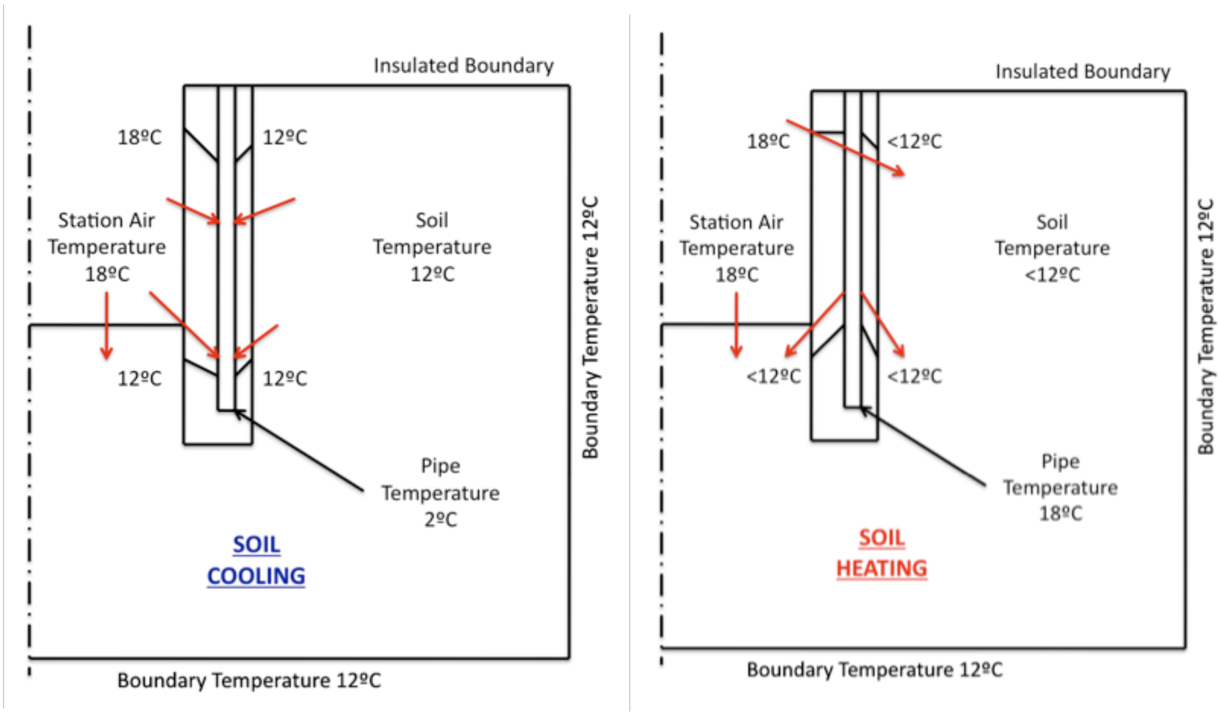


Red arrows show heat flow direction, down the temperature gradients.

**Figure 3.5 – Energy wall seasonal operation. (Not to scale)**

### 3.2.3 Parameter Definitions

The energy wall analysis treats soil as a fully saturated multi-phase continuum, which is characterised by the elastic-plastic Mohr-Coulomb soil model. This model assumes that soil shear strength, $\tau$, increases with increasing normal stress, $\sigma_n$. The shear strength at zero initial stress is the cohesion value, c, and the friction angle, $\phi$, indicates the rate of increase of shear strength with normal stress. The following failure criterion applies:

$$\tau_f' = c' + \sigma_n' \tan \phi$$

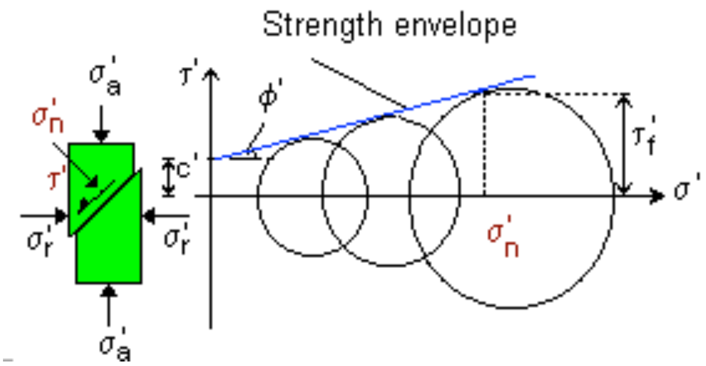


**Figure 3.6 – Mohr Coulomb soil strength envelope.** (Source: University of West England, Bristol)

The initial pore water pressure profile is assumed hydrostatic, with the water table 4m below the soil surface. No dewatering is allowed with suction limited to -100kPa, producing an analysis that tends towards conservative in ground movements, during undrained conditions. The pore fluid is assumed to have a density of 1000kg/m$^3$ and bulk viscosity of 2.2x10$^6$ kg/sm. The initial stress conditions are due to soil weight and hydrostatic pore pressures only, since no surcharge is included in the analysis.

Concrete is modelled as an impervious linear-elastic material. It must be noted that the soil-diaphragm wall interface is modelled as perfectly rough, assuming there will be no relative movement between the diaphragm wall and the soil immediately adjacent to it. The material characteristics of the interface are taken as those of the soil. However, further research is needed to examine the effect of wall friction in reality.

The material properties and characteristics used for the analysis are summarised in Table 3.2 below. All materials are assumed to have isotropic thermal material properties. (N.B. Acceleration due to gravity is rounded up to 10m/s$^2$ for simplicity.)

**Table 3.2 – Material Properties** (Source: Arup Project Documentation)

| Material | Unit | Made Ground | Terrace Gravel | London Clay | Lambeth Group Soils | Concrete** | Steel |
|---|---|---|---|---|---|---|---|
| **Constitutive Model** | | Mohr-Coulomb | Mohr-Coulomb | Mohr-Coulomb | Mohr-Coulomb | Elastic | Elastic |
| **Unit Density (ρ)** | $kg/m^3$ | 1800 | 2000 | 2000 | 2050 | 2500 | 8000 |
| **Elastic Shear Modulus (E)** | MPa | 10 | 90 | 107.25* | 310 | 90000 | 210000 |
| **Poisson's Ratio (ν)** | | 0.25 | 0.2 | 0.2 | 0.2 | 0.2 | 0.3 |
| **Angle of Friction (φ)** | º | 25 | 40 | 24 | 29 | | |
| **Cohesion value (C)** | kPa | 0 | 0 | 0 | 300 | | |
| **Dilation Angle (ψ) *** ** | º | 0 | 0 | 0 | 0 | | |
| **Permeability (k)** | m/s | $8.64 \times 10^{-5}$ | $8.64 \times 10^{-5}$ | $0.86 \times 10^{-9}$ | $0.86 \times 10^{-9}$ | Impervious | Impervious |
| **Specific Heat Capacity (c)** | kJ/(kgK) | 3400 | 3400 | 3000 | 3000 | 3000 | 3000 |
| **Thermal Conductivity (λ)** | W/mK | 1.8 | 1.8 | 1.8 | 1.8 | 2.0 | 2.0 |
| **Coefficient of Thermal Expansion (α)** | $K^{-1}$ | $0.5 \times 10^{-5}$ | $0.5 \times 10^{-5}$ | $0.5 \times 10^{-5}$ | $0.5 \times 10^{-5}$ | $1.3 \times 10^{-5}$ | $1.3 \times 10^{-5}$ |

* This value is averaged with depth of the model for simplicity. In reality E would change with depth for London Clay.

** Scaled to take account of 3D reinforcement within diaphragm wall and slabs.

*** Dilation angle assumed zero to limit shearing at wall-soil interface – limitation of analysis, further explanation in section 3.3.

### 3.3 Analysis Limitations

The energy walls analysis is subject to numerous limitations, both due to need of simplification, and due to limited computational accuracy and resources for the project duration. Therefore, this analysis is only parametric: it allows the investigation of the effects of certain parameters, but it does not give quantitatively exact results. The following limitations apply:

Station Geometry Simplifications

- The station geometry is simplified to 2D, due to limited computational resources. Running the analyses in 3D would require higher resources and time, which were unavailable given the finite project duration. This simplification complicates the creation of an accurate analysis, since the 3D-stiffness-adding propping system cannot be modelled realistically. In terms of consolidation, drainage will occur in 3 directions in reality, as opposed to 2 directions in the model. Furthermore, the simplification hinders the full analysis of the thermo-mechanical effects on the energy wall, since 3D effects may dominate the behaviour of the wall.
- The model used in the analysis is representative of a particular 2D station section only. The results of the analysis are only indicative, and have limited applicability and generalisation to other sections of the station.

- The effects of neighbouring structures on the energy wall are omitted for simplification. The nearby existing London Underground and new Crossrail stations and tunnels could have a major effect on the behaviour of the energy wall. The heat radiated from these sources could affect the thermal regime surrounding the energy wall, therefore affecting its operation.
- The new Crossrail tunnels and over-site developments have not been modelled for simplicity. Their construction could induce settlements and stresses around the energy wall, which are currently ignored.
- The station energy piles, which are in close proximity to the energy wall, are not modelled. However, their operation could affect the temperature distribution around the energy wall. 3D interactions of different thermo-active foundations should be considered in order to obtain a highly realistic analysis.

<u>Soil Modelling Simplifications</u>

- The angle of friction is assumed constant for all types of soil. However, the angle of friction for both made ground and terrace gravel, depends on varying plastic strain.
- The soil dilation angle is assumed zero for the analysis, given computational complications. When the correct dilation angle is used, the plastic strains at the interface between the diaphragm wall and the soil become too large, and therefore unrealistic. If the soil-wall interface were modelled as a slip surface, the correct dilation angle values could be restored.
- The stiffness of clays is assumed constant for this model. However, strain- and creep-rate-dependant stiffness can have a large effect in clays, which would be better represented using the soil BRICK model. This model is a complex elasto-plastic model that incorporates some viscous behaviour components of clays.
- The elastic shear modulus of all soil is assumed constant with depth for simplification. In reality, the shear strength of London Clay will increase with depth, resulting in smaller displacements due to higher soil resistance to shearing.
- No dewatering is included in the construction sequence modelled. In reality, dewatering will be performed to lower the water table below the level of the next excavation. This will change the pore pressure profile, therefore changing the effective stresses in the soil.

- No surcharge is imposed at the soil surface for simplicity. This is unrealistic since the station is in a highly urbanised area and adjacent to a heavily transited road. Furthermore, construction materials and equipment will be placed in close proximity to the excavation, therefore adding a degree of surcharge.
- The soil in the model is assumed fully saturated. In reality, there is an unsaturated zone above the water table, were soil is partially saturated. In this zone, the soil behaviour is more complex than for fully saturated or dry soil.
- Suction is limited to -100kPa for this model. In reality suction may be higher or lower than the specified value, therefore changing the pore pressure and effective stress profiles in the soil.
- The soil-diaphragm wall interface has been modelled as perfectly rough, allowing no relative movement between the soil and the wall. In reality, due to the large difference in stiffness between the soil and the wall, a shear band will progressively form at this interface. The interface should be modelled as a slip surface, however time and computational constraints apply.

Concrete Modelling Simplifications

- The steel reinforcement in the concrete is not modelled (only the shear modulus of concrete is modified to approximate the effect of the rebar on the concrete stiffness). In reality, variations in temperature may cause the rebar to expand or contract, generating differential stresses between the rebar and the concrete, which could change the bending moment regime in the diaphragm wall.
- Concrete is assumed elastic for the entire analysis. In reality, concrete creeps when subjected to long duration loading. Furthermore, if stresses are large, concrete may show decreasing degrees of elasticity.

Thermal Analysis Simplifications

- The diaphragm wall - station air interface has no insulation in the model. In reality, the surface of the wall in contact with the station air will have 200mm of insulation with a conductivity of 0.4W/mK. This will decrease the heat transfer between the energy wall and the station air, therefore the main heat transfer mechanisms will occur between the pipe and the soil only. As a result of this reduction in heat transfer between the station air and the concrete diaphragm wall, the bending moments on the wall due to thermal gradients will reduce.

- The soil surface is thermally insulated. In reality, given the station is constructed adjacent to both Dean St. and Oxford St., the heat recharge due to incident solar radiation on the streets will affect the temperature profile surrounding the energy wall.
- The soil thermal properties are assumed constant for all types of soil, and are taken from general data due to lack of site-specific properties. Therefore, the analysis is only indicative of the general behaviour of the energy wall.
- Thermal properties of the soil are assumed constant for the energy wall model. However, it has been proven that temperature gradients in soil cause moisture migration (Z. Q. Chen et al, 2004). Given that "soil moisture content…greatly changes both the soil thermal conductivity and heat capacity" (A. Alkayssi et al, 2005), a more thorough analysis should include this effect.
- No fluid flow is modelled through the pipe in the diaphragm wall. Modelling the pipe fluid flow would improve the analysis, since it would reflect reality more closely. Furthermore, turbulent or laminar fluid flow impose different heat transfer regimes on the energy wall.
- The way the analysis is run, assumes heat transfer is constant along the length of the pipe in the energy wall, since the temperature of the pipe is set to be uniform. In reality, the heat transfer rate may differ along the length of the pipe.

LS-DYNA Numerical Accuracy

- LS-DYNA has finite numerical accuracy. Its accuracy can be improved using smaller size elements or higher order shape functions, however at a higher computational cost. Furthermore, the simulation timestep size affects accuracy, with too high or too low a timestep introducing inaccuracies or errors.
- The LS-DYNA quasi-static analysis runs by performing regular numerical integrations. This introduces inaccuracies, since a technique known as mass scaling is used to ensure the kinetic energy of the system is kept small to minimize inertia effects. Mass scaling adds non-physical mass to the model, which affects the accuracy of the results.
- Double precision analyses are run in LS-DYNA to minimise the numerical round-off errors, however the improvement of accuracy is limited.

- The energy walls analysis cannot be calibrated, given that there is no in-situ or field data for this particular project. Therefore, the results of the analysis cannot be treated as an exact answer, since no data is available to analyse the accuracy of the results in terms of the real scenario.

## 4.0 Results and Discussion

The results of the Energy Walls analysis are displayed in 4 sections: pore pressures, total and effective horizontal stresses, settlement and displacement, and energy wall bending moments.[4] Due to time constraints, the thermal cycles are applied such that the temperature of the soil changes immediately from the previous state to the subsequent steady state temperature distribution. The soil has an initial homogenous temperature of 12ºC. As the soil is first cooled, the temperature changes immediately from the initial 12ºC, to a steady state temperature distribution in cooling, as shown in Figure 4.0. As the recharge cycle commences, the temperatures change immediately to the steady state temperature distribution in heating as shown in Figure 4.0. Due to low permeability of the clay, thermal equilibrium is reached earlier than pore pressure equilibrium. This analysis shows the worst-case scenario, where temperatures change immediately to the worst steady-state profile. However, further work is required to refine the analysis to a transient state, since the steady state temperatures may never be reached through a period of 6 months in reality.

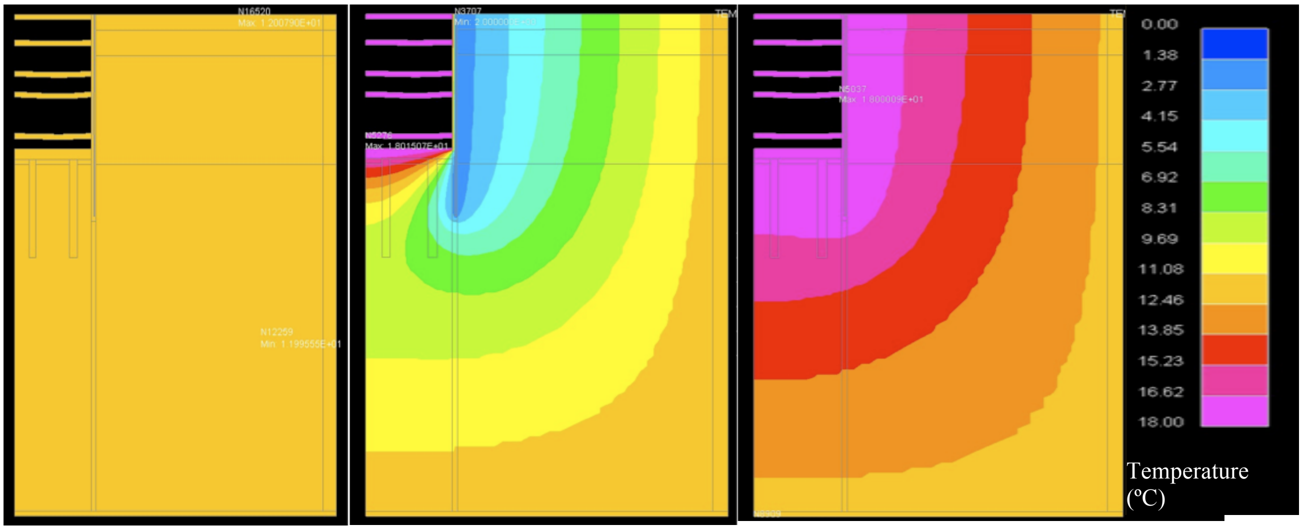


**Figure 4.0 – Temperature contours within model**

**Left: Initial    Centre: Soil Cooling Cycle    Right: Soil Heating Cycle**

---

[4] It must be noted that pore pressure and stress plots show a distinct variation in profiles at depths between 39m and 40m. This is due to end effects and their discussion is ignored for simplicity since it is not relevant for the scope of the project.

## 4.1 Pore Pressure

The initial pore pressure is hydrostatic (with a water table at a level 4m below the surface of the soil) as shown in Figure 4.1. The construction stage analysis is undrained, and as excavation proceeds, the soil surrounding the excavation is sheared. The subsequent behaviour is shown in Figure 4.1, which shows the changes in pore pressure between the start and the end of undrained construction.

Below the excavation, as the soil above is removed, the soil is released from the compression it was subjected to. Given the soil particles and pore fluid are incompressible[5], their volume must remain constant. This means that the decrease in total stress acting on the soil is translated into a decrease in pore pressure (due to decreased volumetric strain on the soil skeleton, and therefore on the pore fluid).  At the sides of the excavation, the horizontal stress in the soil decreases, therefore also inducing a decrease in pore pressure as shown by the lowering contours of pore pressure. (Note that suction has been limited to -100kPa in order to create a conservative analysis. If suction is higher under the base-slab, less heave may occur).

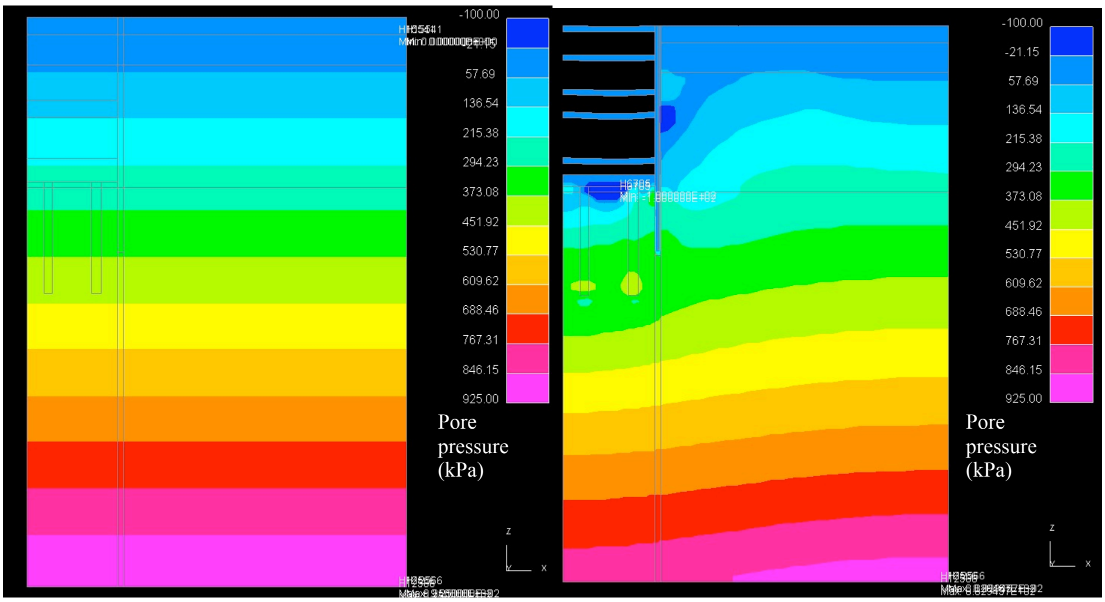


**Figure 4.1 – Pore pressure at start and end of construction**
**Left: Initial Pore Pressures , Right: Pore Pressures at the end of construction**

[5] Even if the pore fluid is compressible, the volumetric stiffness of the pore fluid is much greater than that of the soil skeleton, which has a similar effect as that of incompressibility.

Figures 4.2 to 4.7 show the pore pressure variations in the soil adjacent to the diaphragm wall. These graphs show the initial pore water pressure as the pore pressure when the diaphragm wall was cast (therefore the profile is not hydrostatic).

Figure 4.2 shows the results adjacent to the excavation face of the diaphragm wall. As shown in the figure, at the end of undrained construction, there are no results for pore pressure from the top of the wall to a depth of 28m, since the soil has been excavated. At a depth of 28m (immediately below the base slab) the pore water pressure in the soil has changed due to undrained conditions not allowing the pore fluid to escape. Figure 4.3 shows the results on the diaphragm wall opposite to the excavation face. As shown in the figure, during undrained analysis the pore pressures suffer large deviations from the initial values due to soil shearing and excavation. Suction pressures are generated at depths of 14-19.5m, however these remain small (< -25kPa). Once consolidation starts, the pore fluid drains out of the pores, relieving the excess pore pressures generated during the undrained analysis. This is shown by the pore pressure profiles for 3, 6 and 9 months consolidation, being closer to that of the initial profile in both Figures 4.2 and 4.3. The pore pressures do not return to the exact initial values since consolidation is not complete in 9 months, however most consolidation has occurred at this time.

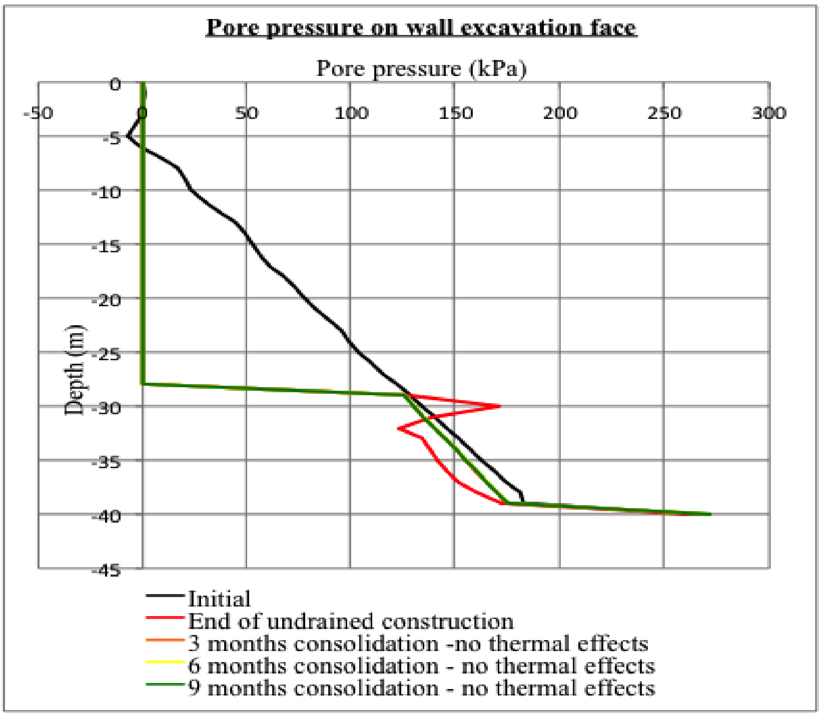


**Figure 4.2 – Pore pressure variation throughout construction and consolidation, on diaphragm wall excavation side**

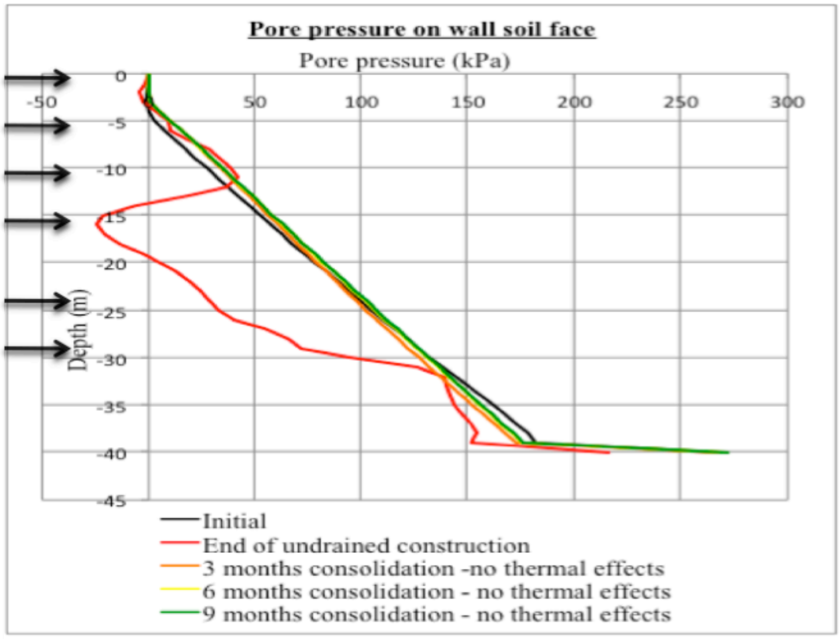


**Figure 4.3 – Pore pressure variation throughout construction and consolidation, on diaphragm wall soil side**

Figures 4.4 and 4.5 show the pore pressure variations due to cooling operation of the energy wall. As the first cooling cycle starts (1 year), the temperature changes immediately from the initial homogeneous 12ºC, to a lower temperature. At the interfaces between the soil and diaphragm wall, the temperature reduces by 10ºC (to a temperature between 2 and 4.15ºC). This decrease in temperature causes the soil skeleton and the pore fluid to shrink, due to the thermal contraction. This contraction decreases the volumetric strain on the soil skeleton and therefore on the pore fluid, causing a decrease in pore pressure shown in both Figure 4.4 and 4.5.

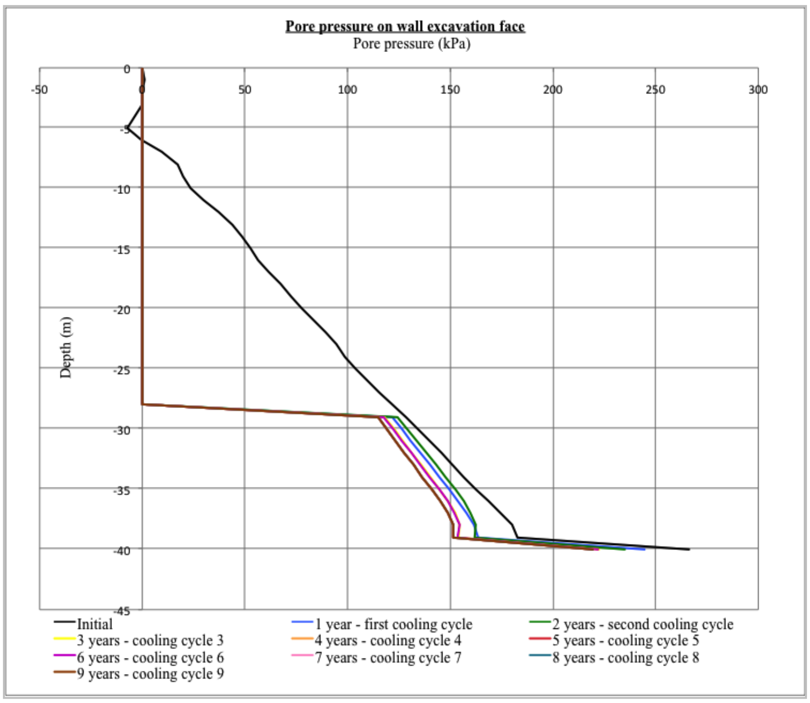


**Figure 4.4 – Pore pressure variation throughout consecutive cooling cycles, on diaphragm wall excavation side**

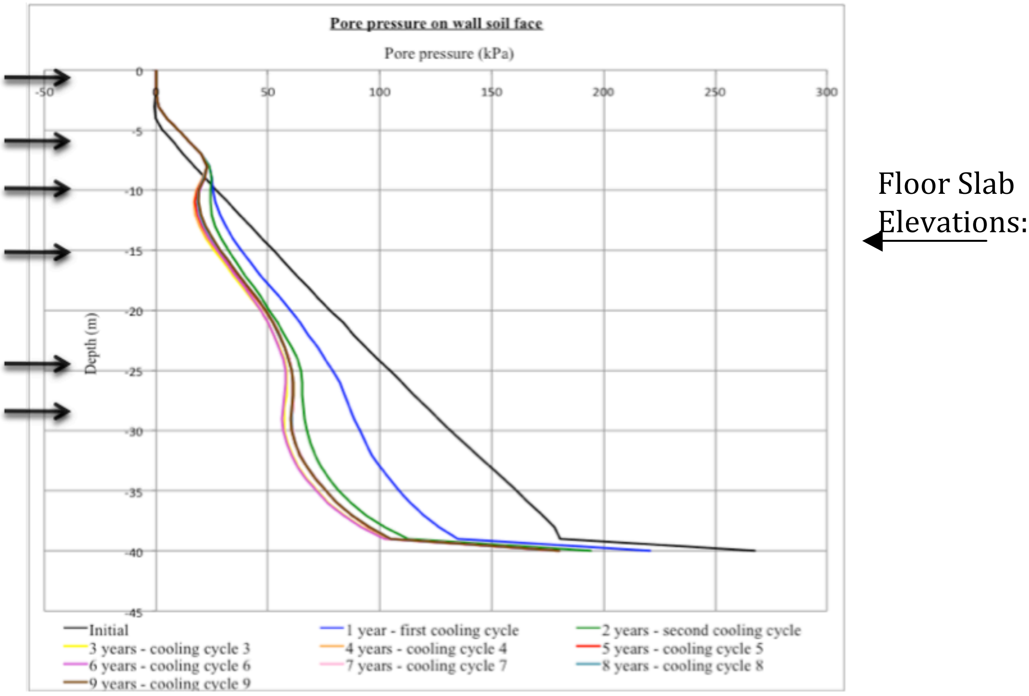


**Figure 4.5– Pore pressure variation throughout consecutive cooling cycles, on diaphragm wall soil side**

For the next cooling cycle the pore pressure reduces much further than for the first cooling cycle as was expected, since the change in temperature is larger: 16ºC change (16.62-18ºC to 2-4.15ºC) as opposed to 10ºC change. The changes in pore pressures resulting from the subsequent cooling stages are each slightly larger than the previous, although the temperature changes for all cycles are the same: 16ºC. Since the thermal expansions are also the same, the volumetric strain induced ($\varepsilon \propto \alpha\Delta T$, where $\alpha$ is the thermal expansion coefficient of the pore fluid) should be the same, therefore inducing the same change in pore pressure. The deviation from what is expected may be due to the temperatures for subsequent cooling cycles not reaching the exact same values as for the previous cooling stage. This effect was observed and documented in P.J.Bourne-Webb et. al. (2009), where it is indicated that this effect is considered to occur "due to the store of thermal mass that has been built up in the extended initial cooling phase". The soil temperatures are disturbed by the initial cooling phase imposing a different change in temperature than subsequent cooling cycles. Therefore, the temperature changes for subsequent cycles cannot represent the behaviour of the undisturbed soil observed in the first cycle. Further work is required to analyse whether this is the case, or whether problems are found within the LS-DYNA code, that do not enable the correct representation of pore fluid expansion[6].

---

[6] Until the end of the project an older version of LS-DYNA was used, which did not model pore fluid thermal expansion correctly. An updated code was installed, which was used to obtain the results included in this report. Given that the code is in constant improvement, there is a possibility that the code is not fully able to represent the exact pore fluid thermal expansion mechanism, therefore owing to unexpected effects such as that explained above.

Figures 4.6 and 4.7 show the pore pressure variations with the recharge cycles of the energy wall. With the first recharge cycle, the temperature of the soil adjacent to the diaphragm wall increases in temperature immediately by 16ºC (from 2-4.15ºC to 16.62-18ºC). This causes thermal expansion of the soil skeleton and pore fluid, which increases the pore pressure. The following recharge cycles cause a larger increase in pore pressure although the temperature changes they induce are the same as the first cycle. Once again, this effect may be due to the "store of thermal mass" as explained previously for the cooling cycles.

Overall, it is apparent that pore pressure does not fully recover through consecutive 6-month cooling and recharge cycles, hence causing an accumulation effect. In reality, the temperature change between previous to steady state will not be immediate. Instead, the temperature will gradually propagate throughout the model over a period of weeks or months, therefore causing more gradual changes in pore pressure. It could be the case that the temperature never propagates to the steady state, therefore smaller temperature differences would occur, inducing smaller changes in pore pressure. This may allow pore pressure equalisation to occur in 6 months, since the changes in pore pressure would be smaller. Further research is necessary to analyse this problem.

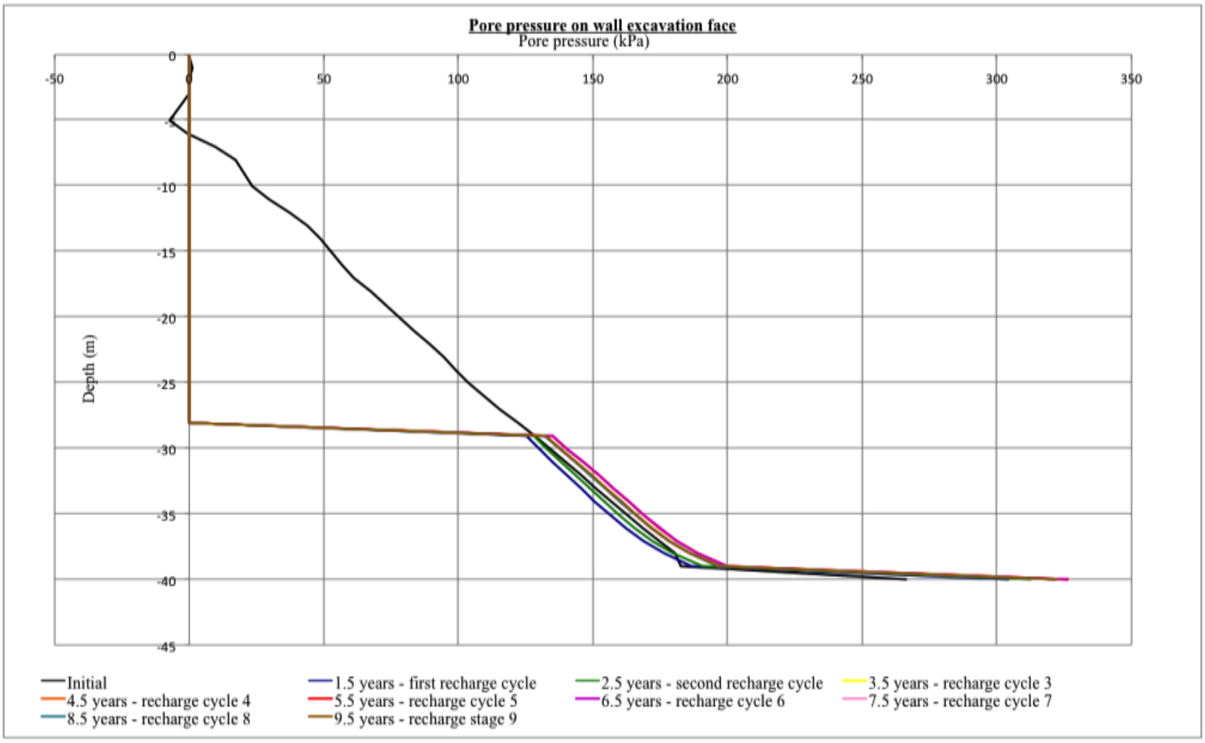


**Figure 4.6 – Pore pressure variation throughout consecutive recharge cycles, on diaphragm wall excavation side**

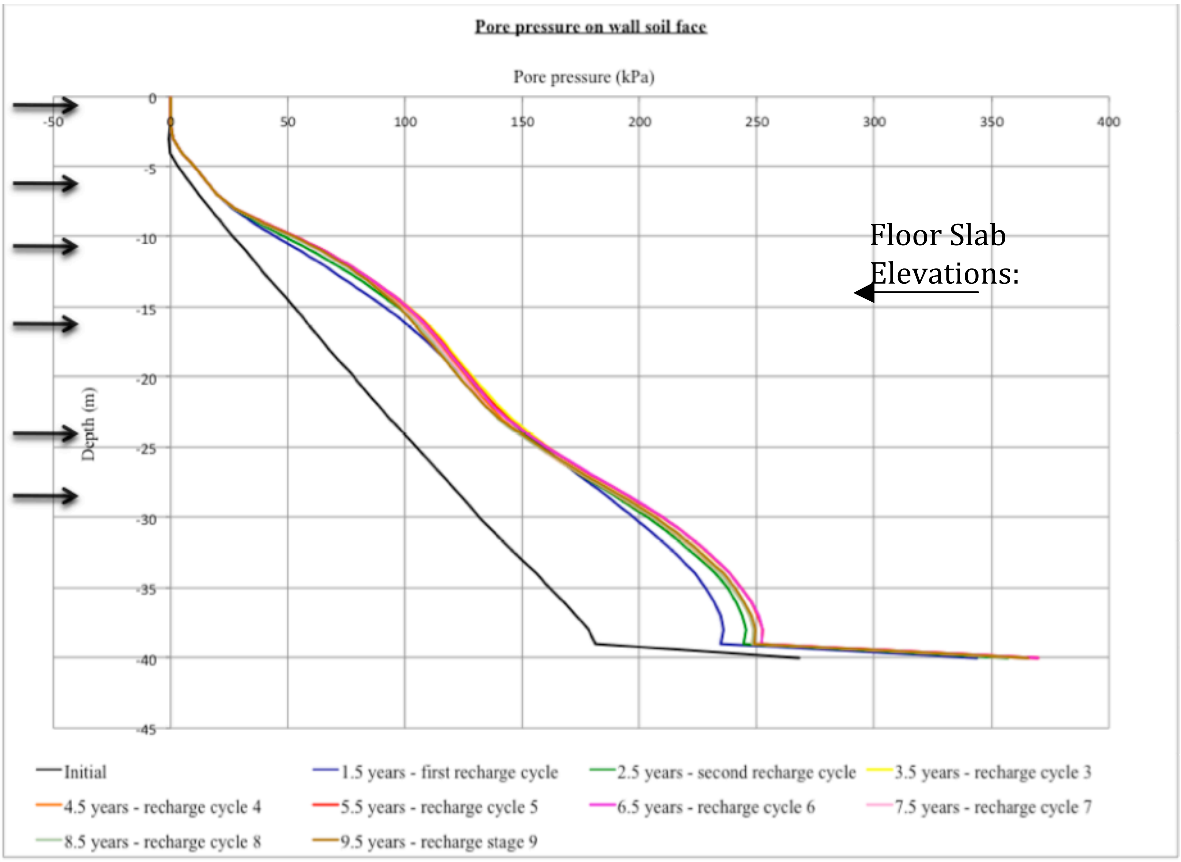


**Figure 4.7– Pore pressure variation throughout consecutive recharge cycles, on diaphragm wall soil side**

### 4.2 Total and Effective Horizontal Stresses

The horizontal stresses in the soil are the most important in terms of diaphragm wall structural behaviour, since these stresses will induce bending moments on the wall.

Figures 4.8 and 4.9 show the total and effective horizontal stresses in the soil adjacent to the diaphragm wall excavation face, through construction and consolidation. The initial total horizontal stress profile in the soil is equal to the vertical stress times the horizontal earth pressure coefficient, therefore the profile is linear. The initial effective stress profile is also linear since it results from the total stress minus the pore pressure, as stated by Terzaghi's principle of effective stresses. The initial profiles shown in Figures 4.8 and 4.9 are not fully linear since they are the profiles when the diaphragm wall is cast. As construction concludes, the stresses from 0m to 28m-depth are zero since the soil has been excavated. From 28m to 40m, the total stress is due to the weight of the soil and the concrete base slab above it. The total stress due to construction changes from the initial state, due to soil excavation and shearing. The effective stress is equal to the total stress minus the pore pressure, thus effective stress also changes from its initial state.

During consolidation, the pore pressures will decrease as drainage of pore fluid is allowed. Since effective stress is equal to total stress minus pore pressure, when pore pressures decrease, effective stress increases as shown in Figure 4.9. Given that total stress is computed as effective stress plus pore pressure, total stress shows the same increase as the effective stress at the end of consolidation. Since the pore pressure is always positive (except in a minor section in undrained), the effective stresses have a larger magnitude than the total stresses at all times. This causes the effective stress profile to be shifted to the left, relative to the total stress profile.

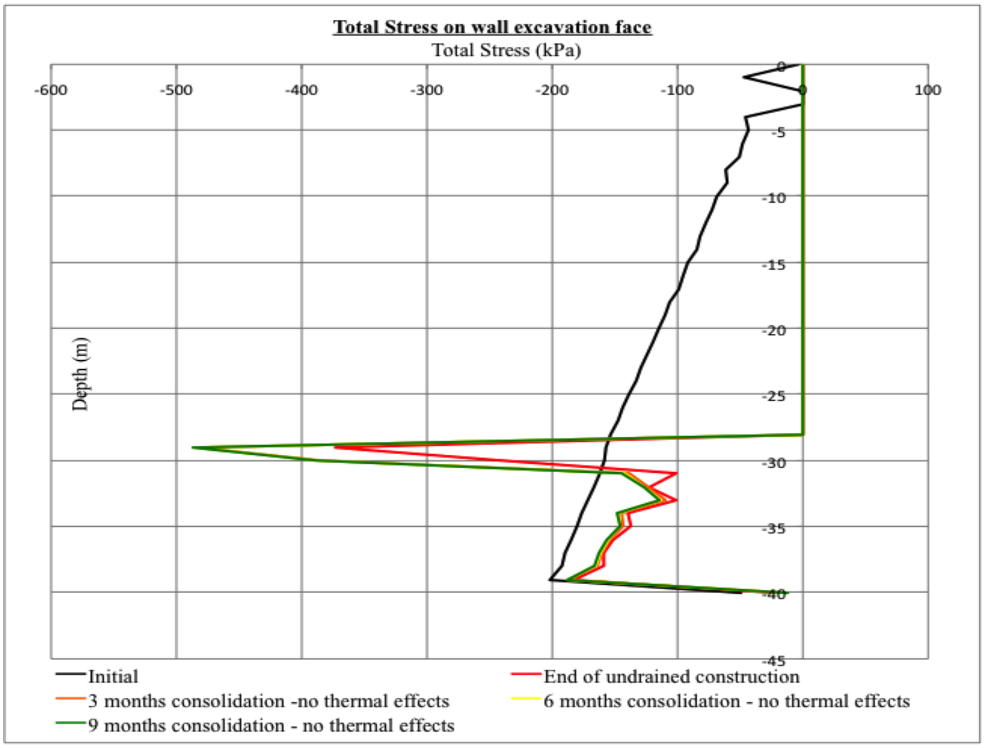


**Figure 4.8 – Total horizontal stress variation throughout construction and consolidation, on diaphragm wall excavation side**

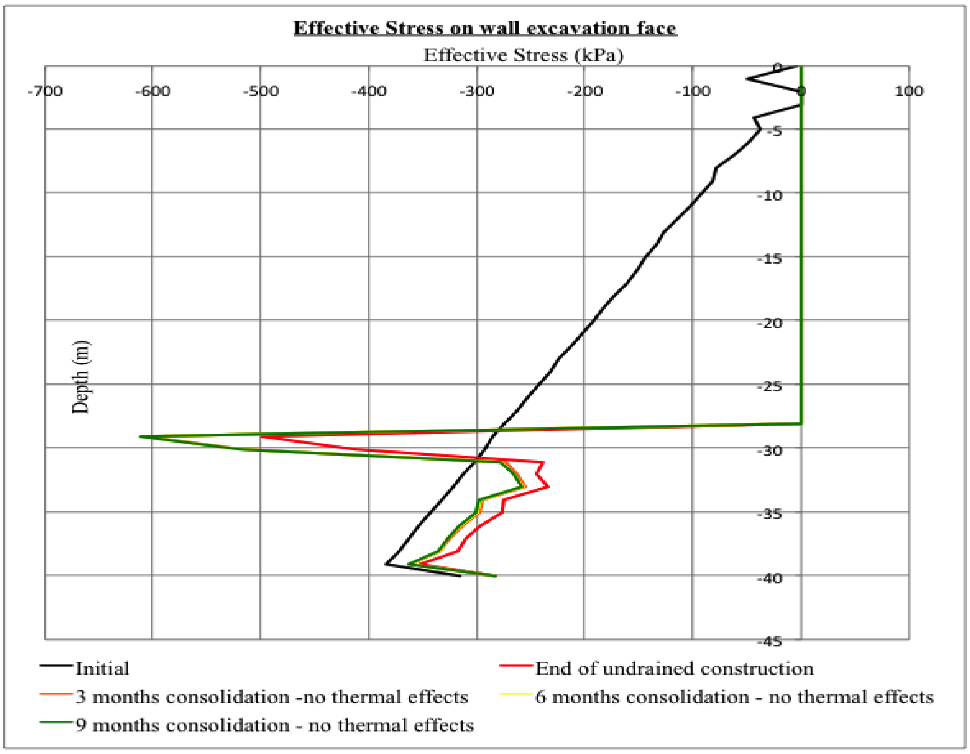


**Figure 4.9 – Effective horizontal stress variation throughout construction and consolidation, on diaphragm wall excavation side**

Figure 4.10 shows the variation of total horizontal stress profiles in the soil adjacent to the diaphragm wall excavation side, due to thermal operation of the energy wall. Due to cooling, the total stress in the soil decreases. This happens because the soil grains and skeleton suffer a thermal contraction, reducing the strain in the soil skeleton. This results in a decrease in total horizontal stress as shown in Figure 4.0. Heating has the opposite effect, since the soil skeleton and grains suffer thermal expansion, thus increasing the stress in the soil.

Figure 4.11 shows the effective stress profile in the soil adjacent to the diaphragm wall excavation face, due to cooling and recharge cycles. Cooling causes soil skeleton and pore fluid thermal contraction, reducing soil skeleton strains and pore pressures. Since the effective stress is equal to total stress minus pore pressure, the effective stress decreases due to the decrease in both total stress and pore pressure. Heating has the opposite effect, therefore causing the effective stresses to increase due to heat recharge.

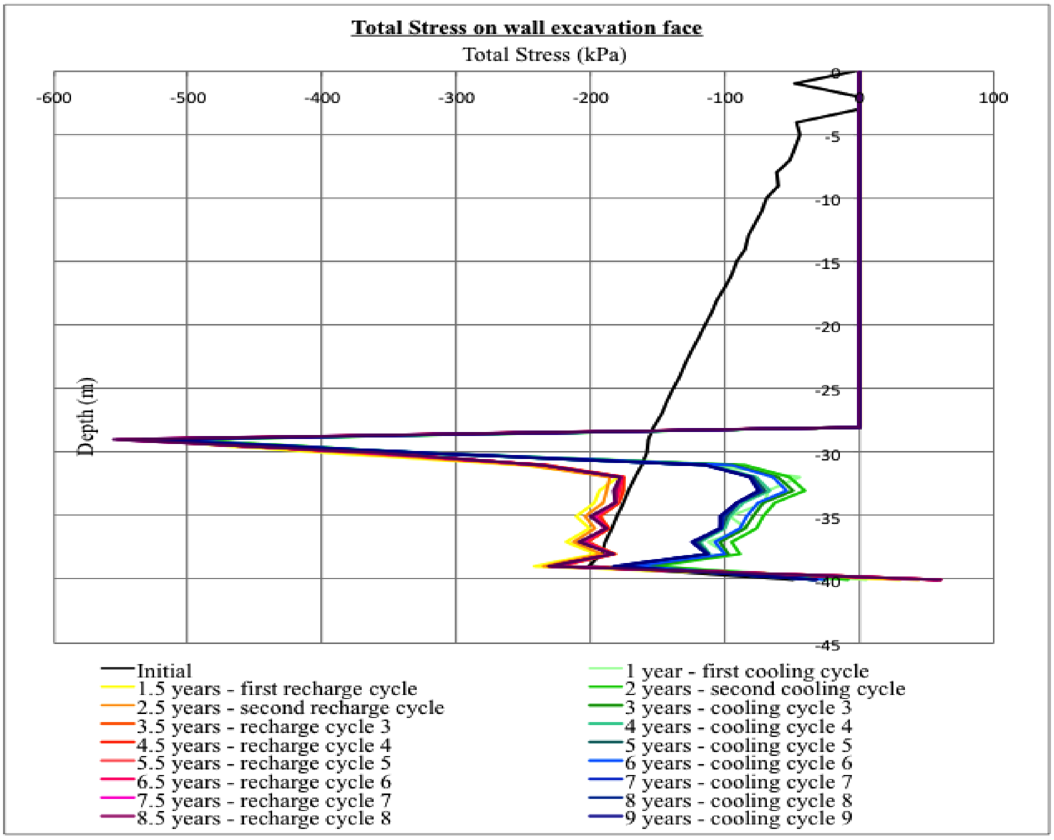


**Figure 4.10 – Total horizontal stress variation throughout energy wall operation, on diaphragm wall excavation side**

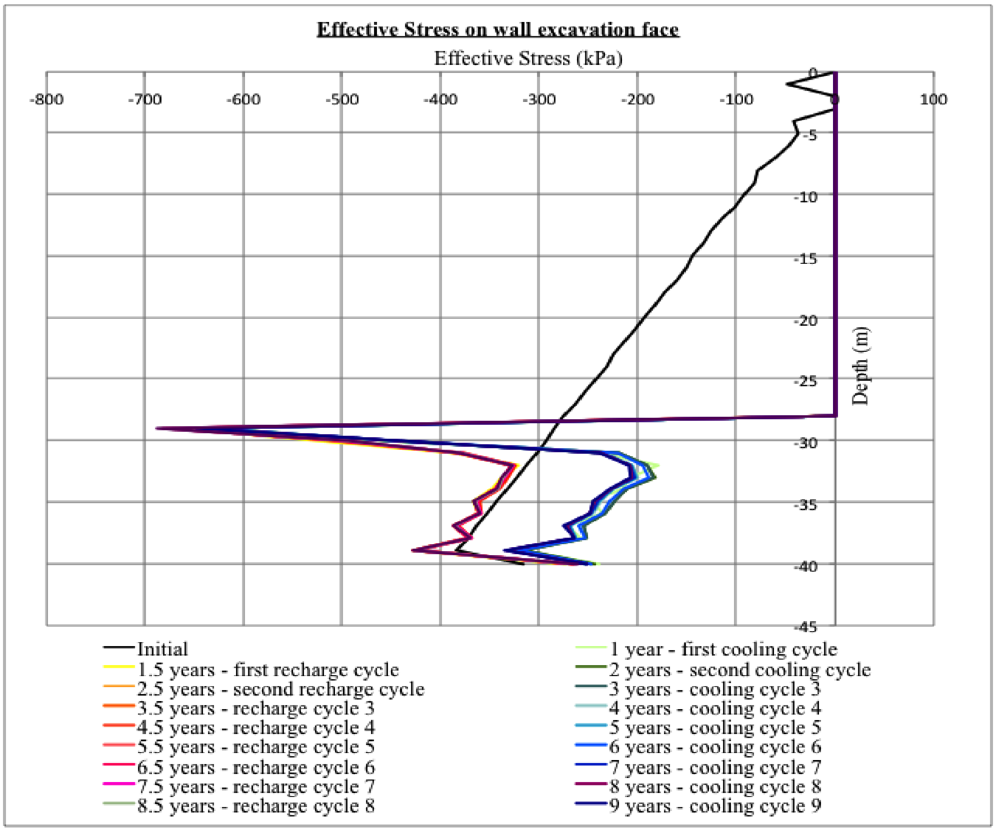


**Figure 4.11 – Effective horizontal stress variation throughout energy wall operation, on diaphragm wall excavation side**

Figures 4.12 and 4.13 show the cumulative total and effective horizontal stresses in the soil adjacent to the diaphragm wall soil face. The initial total horizontal stress is due to the soil weight only, and is therefore linear. As excavation proceeds, the horizontal stresses on the diaphragm wall decrease, and thus it displaces into the excavation. This induces soil shearing behind the diaphragm wall, since the soil "moves" towards the excavation, in the same way as the diaphragm wall displaces. As props and permanent floor slabs are constructed, these exert stresses on the wall, which in turn exert stresses on the soil behind the wall. These changes in stress result in the "zig-zag", highly distorted total stress profile shown. As explained before, the effective stress profile is almost exact to that of the total stress, with the exception that the graph has been pushed towards the left, since effective stress is total stress minus pore pressure. Therefore the highly distorted profiles of effective stress in Figure 4.11 are due to the same phenomena explained for total stress above.

During consolidation, pore fluid drains out of the pores causing a decrease in pore pressure. This corresponds to a decrease in effective stress, and due to Terzaghi's principle, a decrease in total stress.

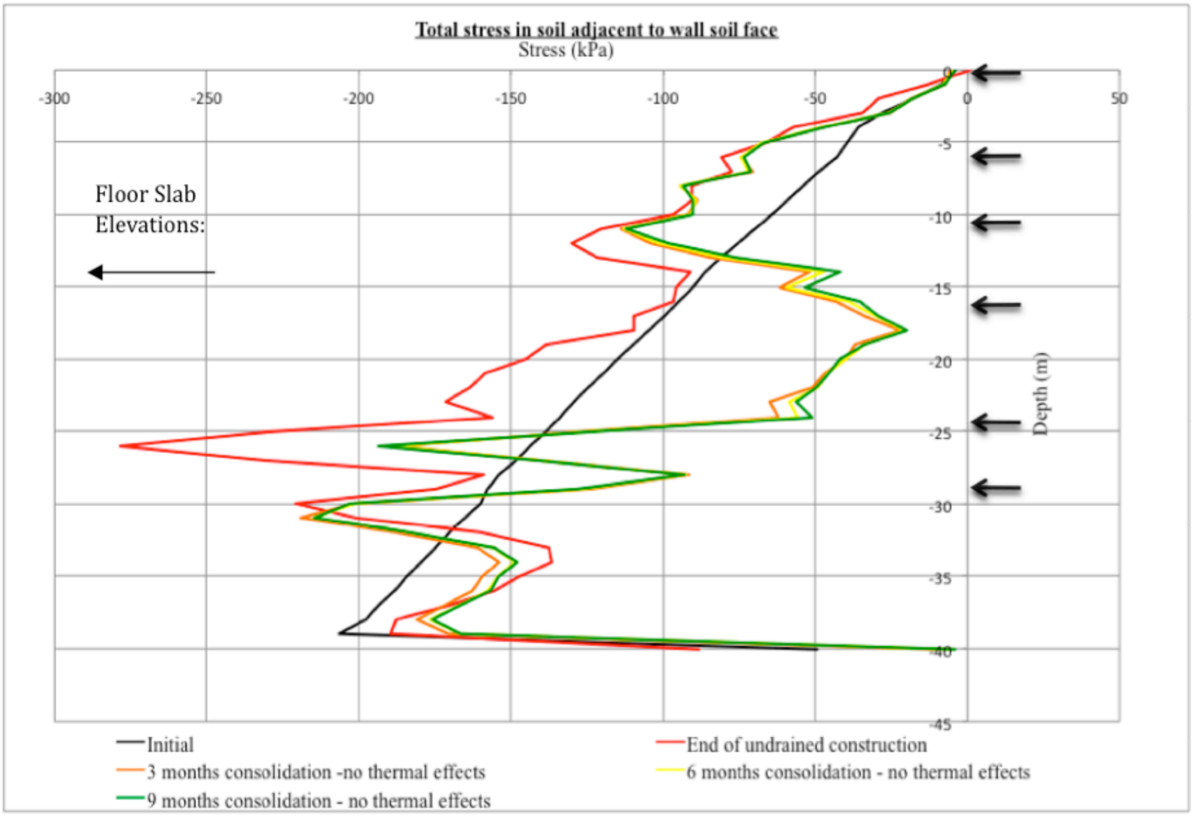


**Figure 4.12 – Total horizontal stress variation throughout construction and consolidation, on diaphragm wall soil side.**
Floor slab locations indicated by arrows.

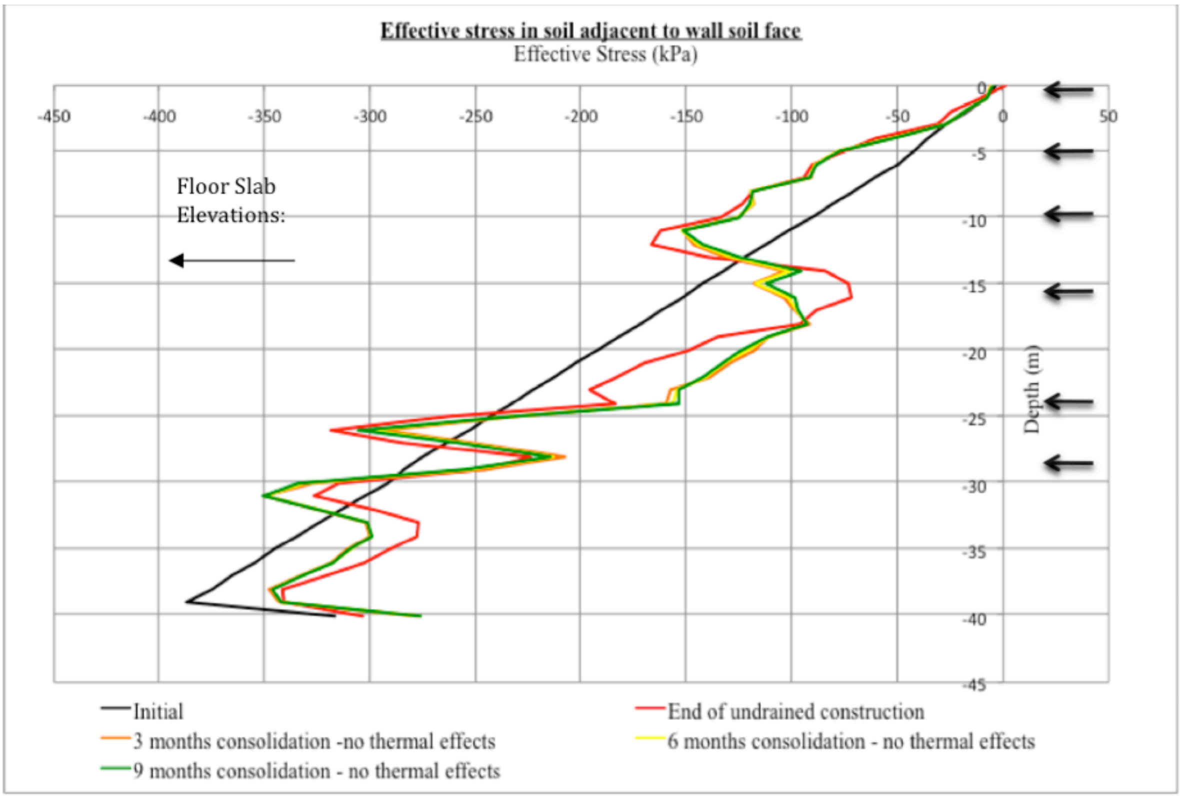


**Figure 4.13 – Effective horizontal stress variation throughout construction and consolidation, on diaphragm wall soil side**

Figures 4.14 and 4.15 show the variation of total and effective horizontal stresses on the soil adjacent to the diaphragm wall soil side, due to energy wall operation. The graph shows the results of cooling cycles in green and blue colours, and those of recharge cycles in orange, red and purple. As cooling occurs, the soil undergoes a thermal contraction, thus decreasing the strain and the stress in the soil skeleton. This induces a decrease in total stress in the soil, as shown by most sections in Figure 4.14. The fact that the total stress increases in some sections is thought to indicate that the soil in that area changes to a passive state, from a previously active state. This may indicate the formation of a pivot about which the diaphragm wall rotates. As heating (recharge) occurs, the soil undergoes thermal expansion, thus increasing the total stress in the soil, as shown by most sections in Figure 4.14. Given that some sections show stresses decrease, instead of increasing, indicates that the soil in that area has gone from an active to a passive state in terms of diaphragm wall operation. Once again, this may show the formation of a pivot, about which the diaphragm wall rotates. Further research is necessary to investigate this effect and its consequences. The effective stress plots show that cooling cycles cause decreases in effective stress, and the reverse in heating (recharge cycles). This is expected due to decreases in pore pressure as explained previously.

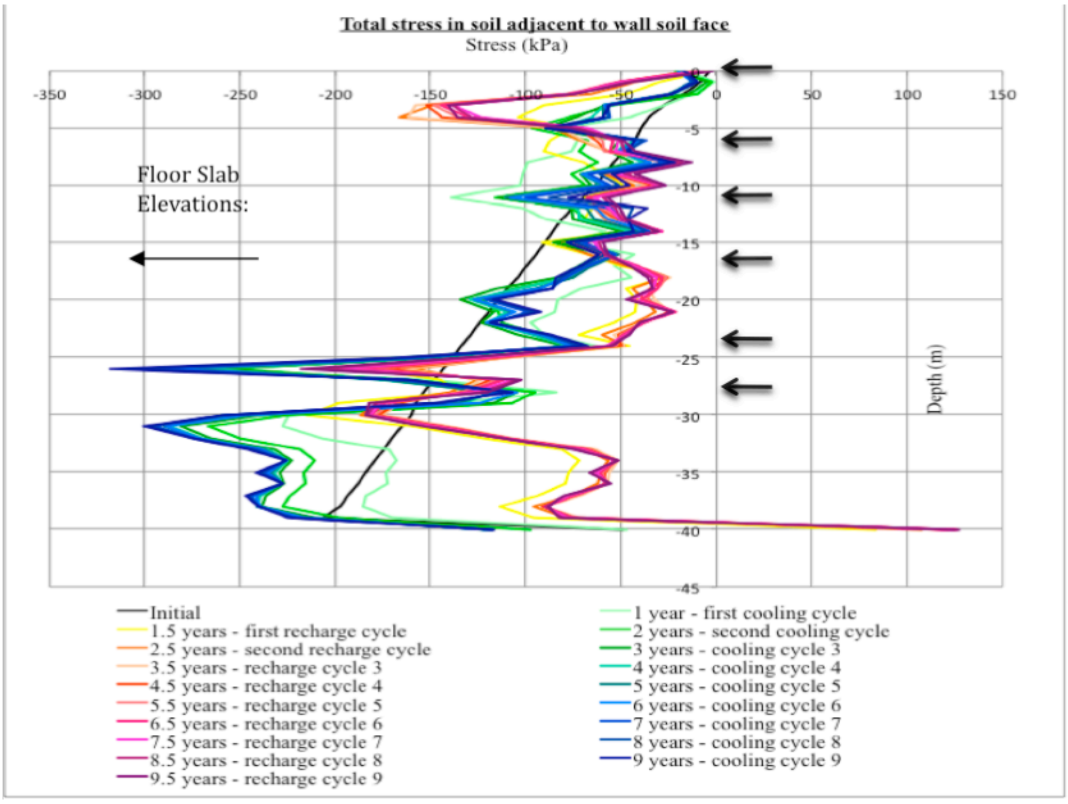


**Figure 4.14 – Total horizontal stress variation throughout energy wall operation, on diaphragm wall soil side**

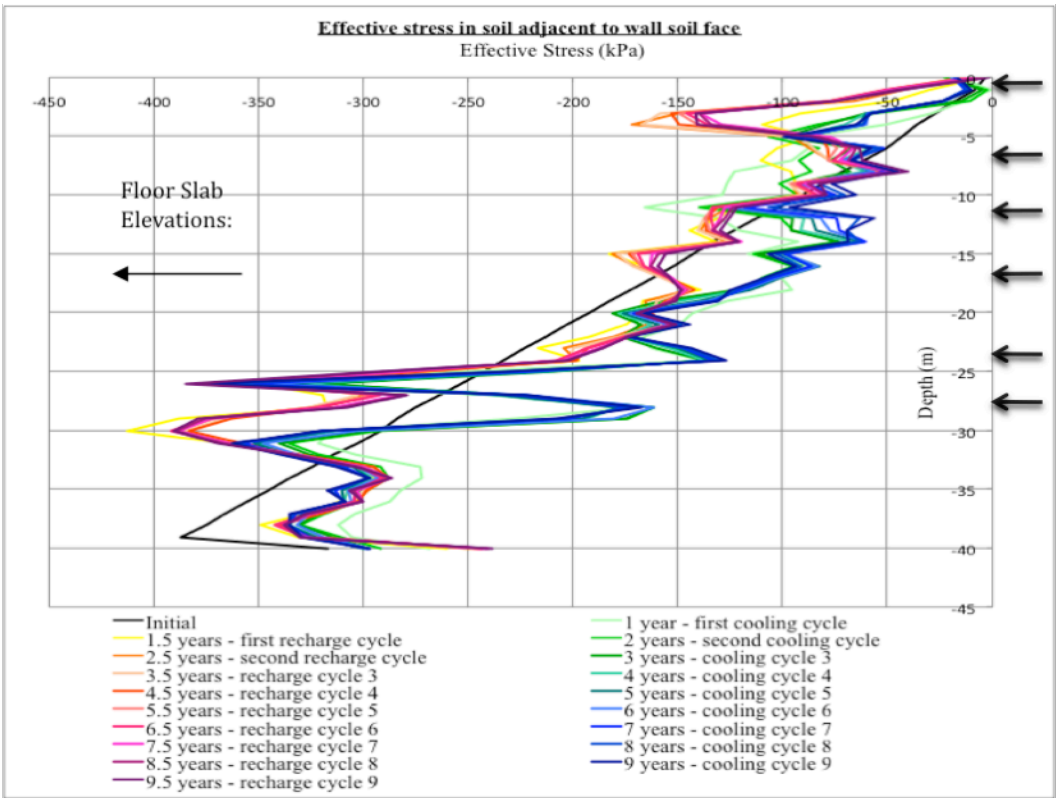


**Figure 4.15 – Effective horizontal stress variation throughout energy wall operation, on diaphragm wall soil side**

## 4.3 Settlement and Displacement

### 4.3.1 Energy Wall Displacement

Changes in pore pressure and thermally induced expansion or contraction of all materials, will cause the soil and the diaphragm wall to displace. Figure 4.16 shows the cumulative horizontal displacement due to construction and consolidation. Negative displacement indicates the diaphragm wall is displacing into the excavation. It must be noted that the “zig-zag” nature of the curve is thought to be due to numerical error introduced by the method of calculation of displacement by LS-DYNA. It is not thought to be a product of mechanical phenomena within the actual model. Further investigation is needed to improve the analysis.

As shown in Figure 4.16, at the end of undrained construction, the wall displaces in a curved manner, with a maximum displacement of 32mm at a depth of 19m. The maximum occurs at this point since this point lies in the area of greatest un-propped diaphragm wall height. The displacement at depths greater than 28m is almost zero since the diaphragm wall toe is embedded in 12m of soil. The magnitude and shape of the displacement are thought to be correct and acceptable for construction-induced displacements, since they fit predictions from Arup (Analysis of Dean Street Station, Arup 2010-2011). Consolidation causes a further 2.5mm increase in movement (maximum) due to pore fluid draining from the pores, therefore resulting in a change in volume of the soil matrix.

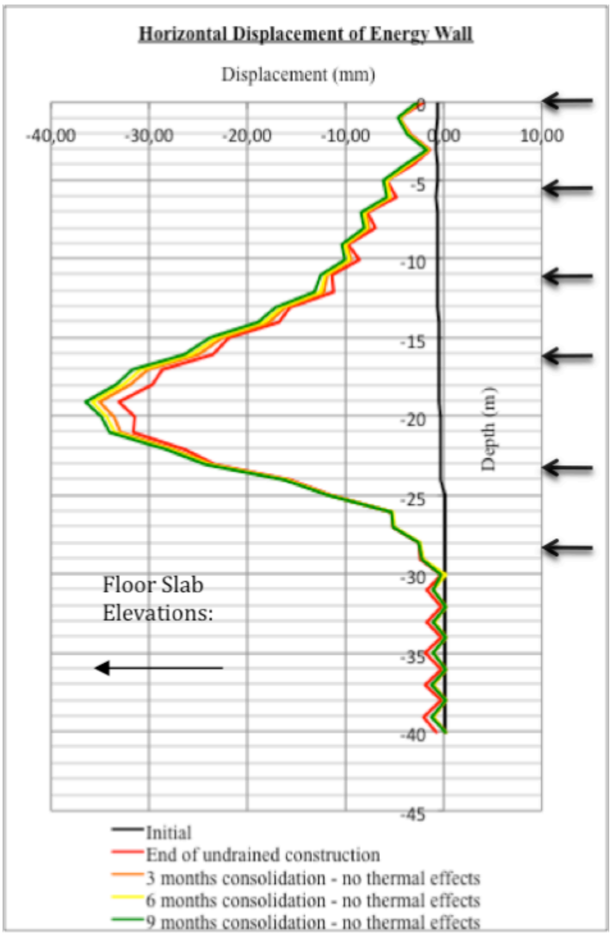


**Figure 4.16– Horizontal displacement of diaphragm wall due to construction and consolidation.**

As shown in Figure 4.17-1, with a cooling cycle, the temperature decreases by 16ºC, and the soil shrinks due to cooling. This causes the displacement of the wall to decrease by 1mm relative to the cumulative displacement at the end of the previous recharge cycle. As the excess pore pressures dissipate during the cooling cycle, the displacement increases by a further 2mm. After the recharge cycle starts, the soil expands due to heating, as the temperature increases by 16ºC. Increasing temperatures increase the hydraulic conductivity of the pore fluid, facilitating drainage and therefore increasing displacement slightly, for a given recharge cycle as shown. These effects in conjunction cause the diaphragm wall to displace by around 5mm more in heating than in cooling. Since the analysis is a coupled thermo-hydro-mechanical analysis, the changes in displacement due to thermal stresses and dissipation of pore pressures cannot be fully differentiated. Further investigation would be necessary to analyse the relative contributions of each effect.

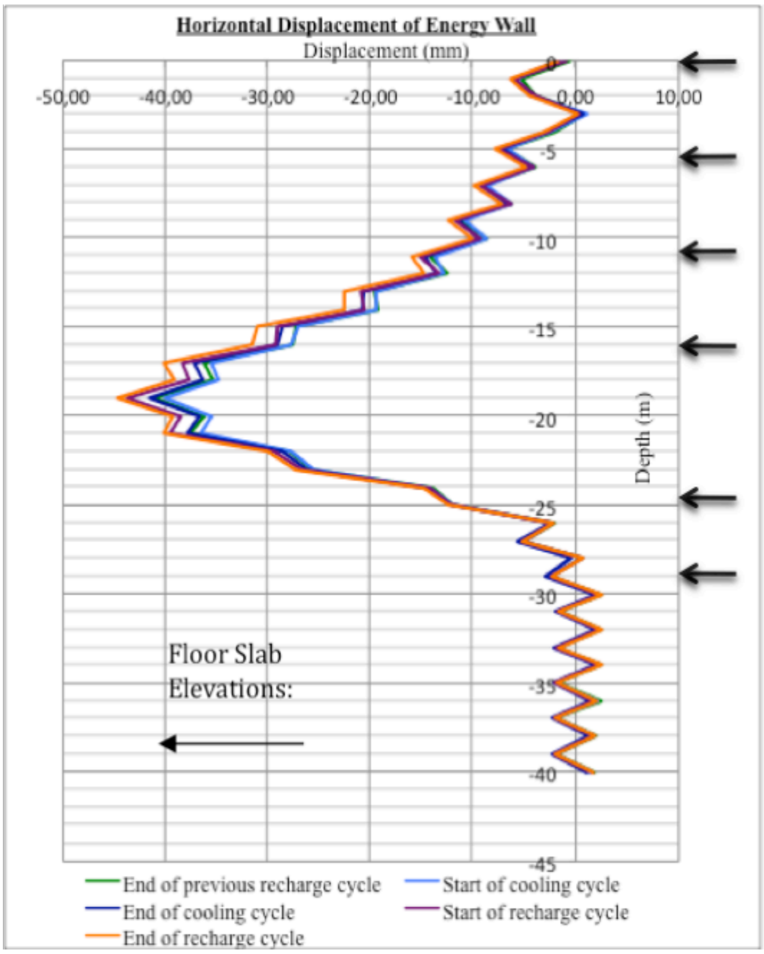


**Figure 4.17-1– Horizontal displacement of diaphragm wall due to cooling and recharge operation.**

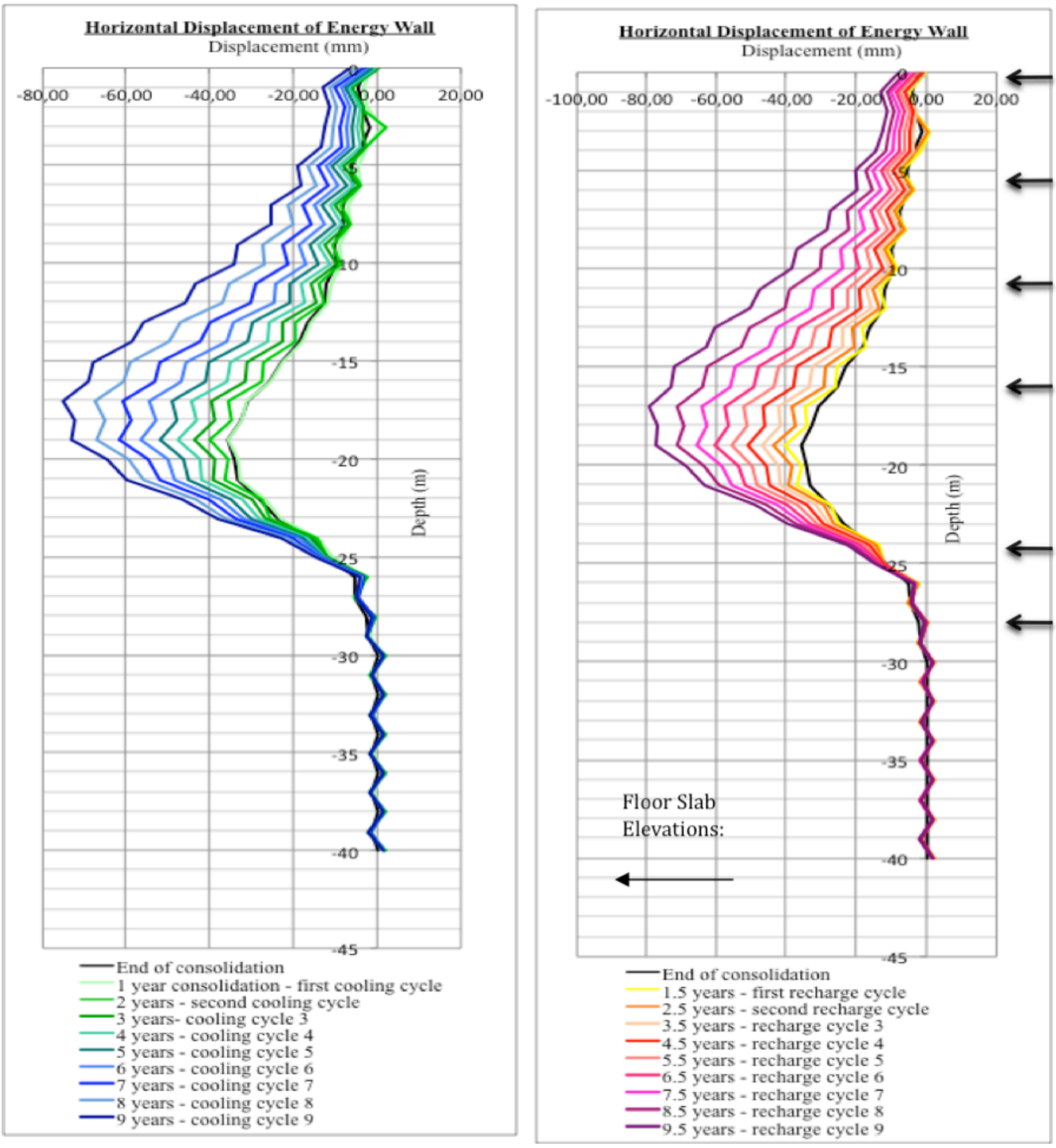


**Figure 4.17-2– Horizontal displacement of diaphragm wall due to energy wall operation. Left: Displacement due to cooling cycles. Right: Displacement due to recharge cycles.**

The displacements due to consecutive cooling and heating cycles are larger than the previous respective cycles. Given that the soil is elasto-plastic, it was expected that the soil would not return to its original position, however this increasing change of displacement for every consecutive cooling or heating cycle was not expected, given that the magnitude of the temperature change is always the same.

Although the total displacement after 9 years is acceptable: 85mm, it is alarming that the displacement change due to each cycle increases. Given that the pore pressures do not recover to the expected states, as explained in section 4.1, an accumulation of pore pressures occurs. The effective stresses depend on the pore pressure; therefore they manifest a similar accumulation effect. It seems that this accumulation effect in pore pressures and effective stresses can be the cause of magnification in displacements due to consecutive thermal cycles. Given that in reality there will be insulation on the excavation side of the diaphragm wall, the temperature gradient between the diaphragm wall and the soil will be smaller. This means that the expansion of the pore fluid and soil skeleton will decrease, reducing changes in stresses and pore pressures, which will lead to smaller displacement. However, further research is necessary to analyse this effect in depth.

### 4.3.2 Soil Surface Settlement

The settlement of the soil behind the diaphragm wall is shown in Figures 4.18 to 4.20. Horizontal displacement and settlement are highly interlinked, since the horizontal displacement of the wall into the excavation will cause the soil to move towards the zones of most displacement of the diaphragm wall. Pore pressures and thermal stresses are the main factors influencing the settlement of the soil surface.

Initially, the soil is assumed level. As indicated in Figure 4.18, construction is analysed as undrained and therefore pore pressures cannot dissipate. As excavation proceeds, the diaphragm wall displaces horizontally due to relieved horizontal stress. This allows the soil to "flow" towards the left, filling the space the diaphragm wall left empty as it displaced. This phenomenon causes settlement behind the diaphragm wall. The shape of the settlement curve is thought to be a result of the soil "flow" mechanism, causing maximum displacement at 30m from the diaphragm wall. It must be noted that the settlement at 0m behind the diaphragm wall is 0 due to the rough boundary modelled between the wall and the soil, which allows no relative movement of both. The maximum settlement at the end of construction is 16mm, which is within acceptable limits of settlement. As consolidation occurs, excess pore pressures are relieved, which allows the soil to swell upwards, therefore decreasing settlement slightly to a maximum of 15.5mm.

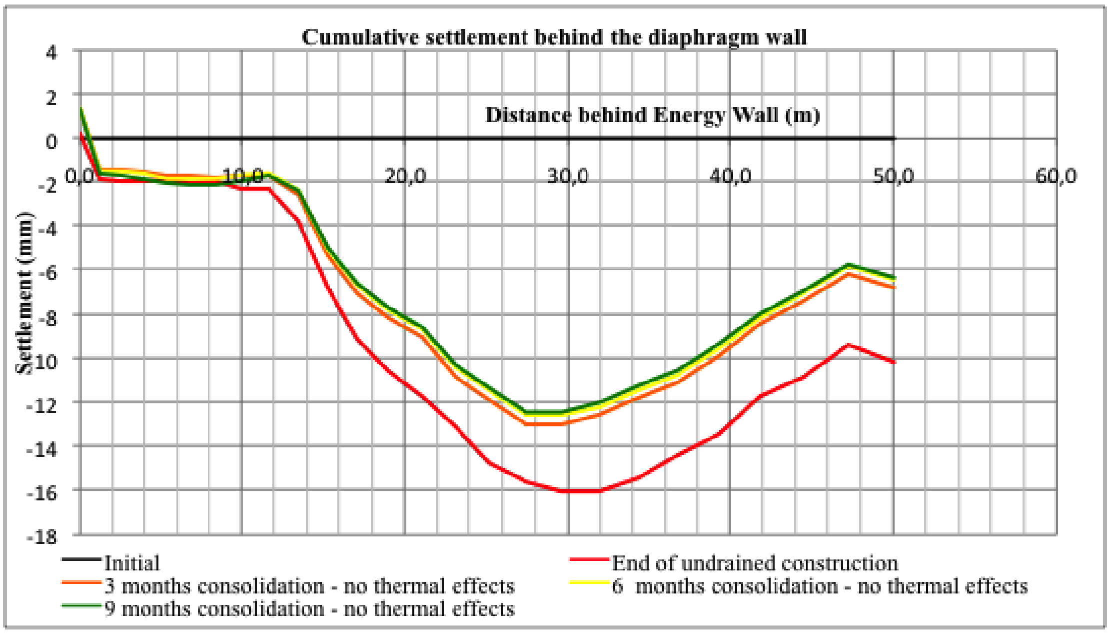


**Figure 4.18 – Settlement behind the diaphragm wall due to construction and consolidation.**

When the first cooling cycle starts, the temperature of the soil reduces by 10ºC, causing the soil to shrink and pore pressures to decrease. As shown in Figure 4.19, this causes an increase in settlement of 8mm (maximum). Settlement increases most, closer to the diaphragm wall, since the temperature drop is highest at this location. As the distance behind the wall increases, the increase in settlement decreases due to higher temperatures in these sections (i.e. temperature change between the previous and current state in these sections of the soil is smaller).

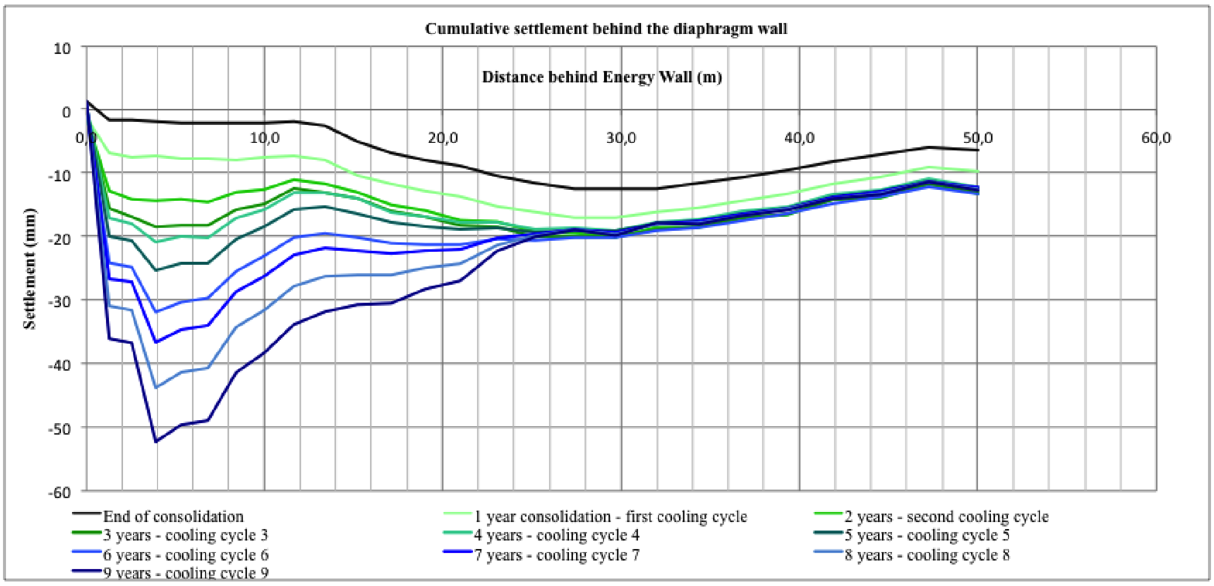


**Figure 4.19 – Settlement behind the diaphragm wall due to consecutive cooling cycles.**

As shown in Figure 4.20, with the start of the first heating cycle, the soil skeleton and pore fluid expand, which causes the soil to swell. Given that the temperature change is 16ºC, the magnitude of change in settlement due to heating is larger than that for cooling (change in temperature for first cooling cycle was 10ºC). Once again, the change in settlement is most pronounced closest to the energy wall, given that the temperature gradients are highest in this area. These will cause larger changes in strains, thus larger settlements.

The consecutive cooling and heating cycles cause the settlement to increase to a maximum of 54mm after 9.5 years of operation. This values is acceptable, however the fact that consecutive heating and cooling cycles show increasing magnitudes of changes in settlement is alarming. This effect may be due to the fact that pore pressures do not recover during 6 months of cooling or heating, causing pore pressure accumulation. This, in turn will cause a magnification in settlement between consecutive heating and cooling cycles. Further investigation is needed to analyse the effect of this phenomenon on the long-term operation of the energy wall. A concern arising from this analysis is that displacements of the diaphragm wall and settlements of the soil surface will increase progressively due to energy wall operation, throughout the lifetime of the structure.

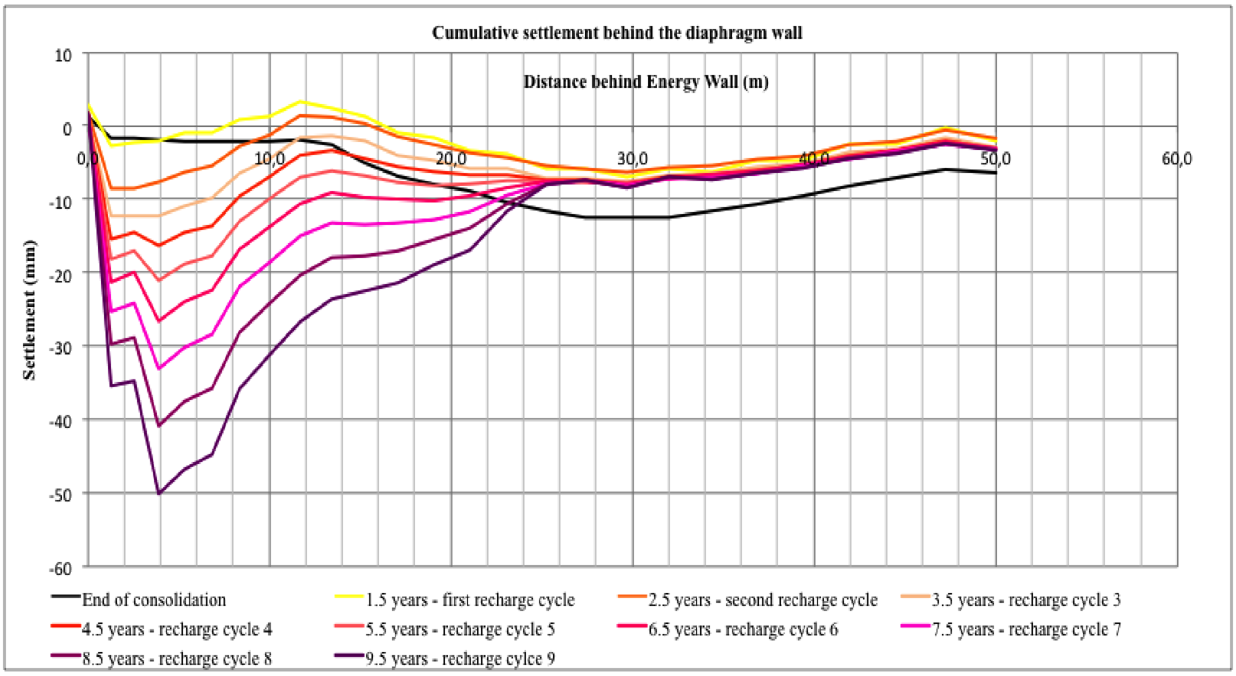


**Figure 4.20 – Settlement behind the diaphragm wall due to consecutive recharge cycles.**

## 4.4 Energy Wall Bending Moment

Construction and consolidation cause stress and strain variations in soil, and thermal operation of the energy wall cause stress and strain variations in both concrete and soil. Therefore, differential strains can develop within the width of the diaphragm wall, which induce bending moments in the wall. The thermal expansion or contraction of concrete causes a variation of volumetric strains within the diaphragm wall. Given that the temperature within the width of the wall is not uniform, since the pipe is not centrally-located, and that the wall is restrained from moving by the soil and the concrete floor slabs, the differential strains induce a bending moment on the wall. The thermal expansion or contraction of the pore fluid and soil skeleton causes a change in pore pressures, total stresses and effective stresses in the soil. Therefore, soil pressures acting of the wall change, causing further bending moments. Once the pore pressures dissipate after the temperature cycle starts, this causes a further stress redistribution, leading to further changes in bending moment. The overall effect of these phenomena in conjunction is observed in Figures 4.21 and 4.22. Further work is required to obtain an analysis indicating the effect of each contribution separately.

As shown in Figures 4.21 and 4.22, the bending moment is smallest at the bottom 8m of the diaphragm wall since this is the toe of the wall, and it is well embedded into the soil. Between 0m and a depth of 15m the bending moments remain within a maximum magnitude of 900kNm, which is small compared to the maximum magnitude of the bending moments at -19m: 2550kNM, and at -25m: 3500kNm. This is because the top section of the diaphragm wall is restrained by more closely-spaced floor slabs compared to the bottom. The bending moment at -19m is large since this point is in the section of diaphragm wall with least horizontal restraint, therefore the wall is allowed to bend the most. The bending moment at 25m-depth is large due to the high stiffness of the base slab causing a high force on the diaphragm wall, which in turn imposes a large bending moment.

A positive result is that the bending moments due to any stage of the analysis remain within the maximum bending moment envelope determined by Arup (based on the plastic moment capacity of the wall). There are two exceptions to this statement: at the top 3m of wall and at a depth of 24-26m. The top deviation may be due to the fact that the top floor slab modelled does not provide sufficient restraint for the wall compared to reality. At a depth of 24-26m, the deviation is due to positional tolerances of the floor slab in this area. The Hypermesh model created for the Energy Wall was limited to having 1m thick elements, and therefore only being able to place floor slabs at full number depths (i.e. 23m not 23.2m), even though in reality this is not the case. Furthermore, the bending moment in the wall surpasses the safe bending moment envelope determined by Arup, only after 7 years of operation at a depth of 25m to 27m. This may be partly due to positional tolerance, however the general trend of highly increasing bending moments is alarming. Once again, this increase of bending moment is due to the accumulation effect mentioned previously, and therefore further research is necessary to analyse this effect. Further investigation is required to obtain a quantitative analysis of the bending moments imposed on the wall by the short and long-term operation. This would allow setting upper bounds to the bending moment that the diaphragm wall can resist if it is to remain safe during thermal operation.

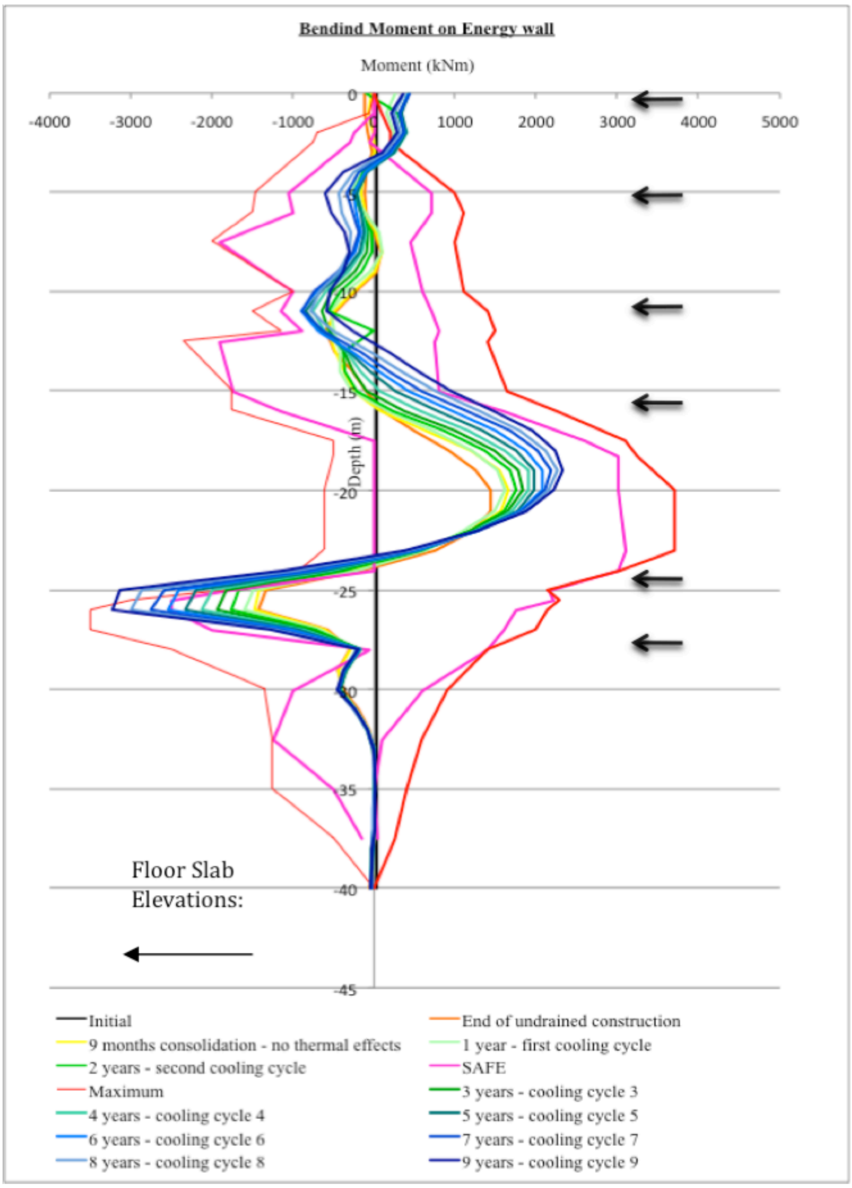


**Figure 4.21 – Bending moment on diaphragm wall through construction and consecutive cooling cycles.**

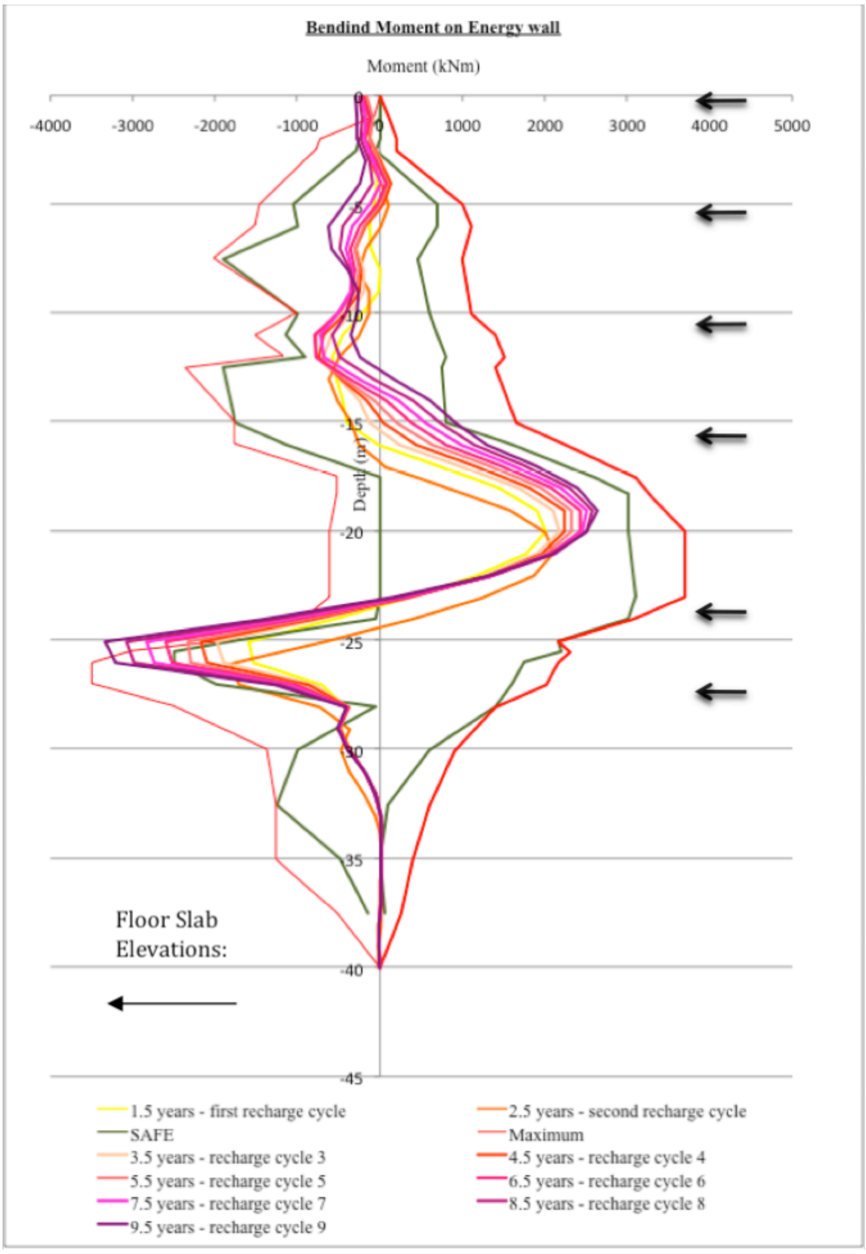


**Figure 4.22 – Bending moment on diaphragm wall through construction and consecutive recharge cycles.**

## 5.0 Conclusions

The thermal operation of the energy wall causes changes in pore pressure, total stress and effective stress in the soil. These, in turn, cause displacements of the diaphragm wall into the excavation, changes in settlement and variations of the bending moments on the diaphragm wall.

During cooling operation, the soil skeleton shrinks due to thermal contraction, which decreases the total stress in the soil. Due to volume conservation, the shrinking of the soil skeleton subjects the pore fluid to increased compressive volumetric strains. These reduce the pore pressures in the soil; therefore the effective stresses in the soil decrease. As a result, the displacement of the diaphragm wall decreases, and soil surface settlement increases due to soil matrix contraction. During the 6 months of cooling, excess pore pressures are allowed to dissipate, causing the soil to swell, which reduces settlement but increases diaphragm wall horizontal displacements. Furthermore, differential thermal stresses within the diaphragm wall cause differential strains, which induce bending moments on the wall. The total bending moment on the diaphragm wall due to cooling is due to variations in stresses and thermally induced bending moments within the diaphragm wall.

During heating (recharge) operation, the reverse to cooling occurs. Temperature increases cause the pore fluid and soil skeleton to expand, increasing pore pressure, effective and total stresses. These cause an increase in diaphragm wall horizontal displacement, and a decrease in settlement due to soil matrix expansion. Thermal expansion of the diaphragm wall itself induces bending moments on the wall, which add to the bending moments due to soil pressures. Heating cycles induce greater displacements than cooling cycles since increasing soil temperature increases the hydraulic conductivity of the soil, therefore increasing displacements due to pore pressure recovery.

The main concern raised by this analysis is the magnification of displacement, settlement and bending moment changes with consecutive thermal cycles. If these parameters increase steadily throughout the thermal operation of the energy wall, the safety of the geotechnical structure will be threatened at a point throughout its lifetime. It is thought that the cyclic thermal behaviour of the energy wall may cause soil strength degradation, compromising the structural performance of the diaphragm wall. For this reason, extensive investigation of the thermo-hydro-mechanical behaviour of energy walls is required, in order to evaluate their long-term stability and confirm their safety for continued use.

## 6.0 Suggestions for Further Work

Given the limitations of the Energy Walls analysis explained in section 3.3, there is room for improvement and further work. The most important further work suggestions are summarised below:

1.0 Analysing whether the bending moments resulting after immediate heating or cooling are due to thermally induced stresses, or due to varying soil pressures as the pore pressures change.

2.0 Perform an improved 2D thermo-hydro-mechanical analysis by imposing specified heat fluxes or heat extraction requirements, as opposed to setting pipe temperatures.

3.0 Performing a complete 2D transient coupled thermo-hydro-mechanical analysis of the energy wall, with a daily and annual variation of temperature at the top surface of the soil.

4.0 Implementing the advanced elasto-plastic soil BIRCK model for clays in a 2D analysis, which reflects the clay soil characteristics more appropriately compared to the Mohr-Coulomb model.

5.0 Extending the 2D analysis by the use of a more advanced or modified versions of the BRICK and Mohr-Coulomb soil constitutive models, to model the viscous behaviour of soil. This would allow the investigation of the effects of creep.

6.0 Extending the 2D analysis further, to model the long-term behaviour of the Energy Wall over a period of 50 years of uninterrupted operation.

7.0 Performing a coupled 3D thermo-hydro-mechanical analysis of the energy wall, consecutively adding all the improvements mentioned above.

8.0 It would be highly advantageous to install monitoring and measuring devices into newly constructed energy walls, in order to obtain field data that would enable computational model calibration.

9.0 Further investigation of the effect of thermally induced strains and stresses on both soil and diaphragm wall is necessary. This would allow the determination of limiting stress and strain values, which could be monitored using appropriate instrumentation during the operation of the energy wall, in order to ensure that the system will remain safe.

## Appendix

### A.1 Risk Assessment Retrospective

The project's initial risk assessment poorly analysed the severity of some of the risks involved. It mainly considered risks related to ergonomic design of the workspace and posture, however the impact of these risks was not evaluated efficiently. Only through repeated use of the workspace, did it become apparent how severe the impacts of inadequate posture and poor workspace layout were. Furthermore, the likelihood of occurrence and impact of tripping hazards resulted higher than expected, not only in the main workspace, but also in its access route. Visual strains due to glare and insufficient lighting intensity resulted in a major aspect of discomfort and poor attainment at specific times, as did insufficient ventilation and air freshness in the workspace. In retrospect, a thorough and complete risk assessment should have been completed through the use of the designated workspace, not merely through reasoning and past experience, as was the case for the initial assessment. The risk assessment should have indicated all the risks, their likelihood of occurrence and impact, as well as corresponding remedial or mitigating actions. In cases were the impact of the risk seemed subtle, this should have been evaluated in terms of its effect to productivity and comfort, which are closely related to attainment and therefore project success.

### A.2 Project Programme

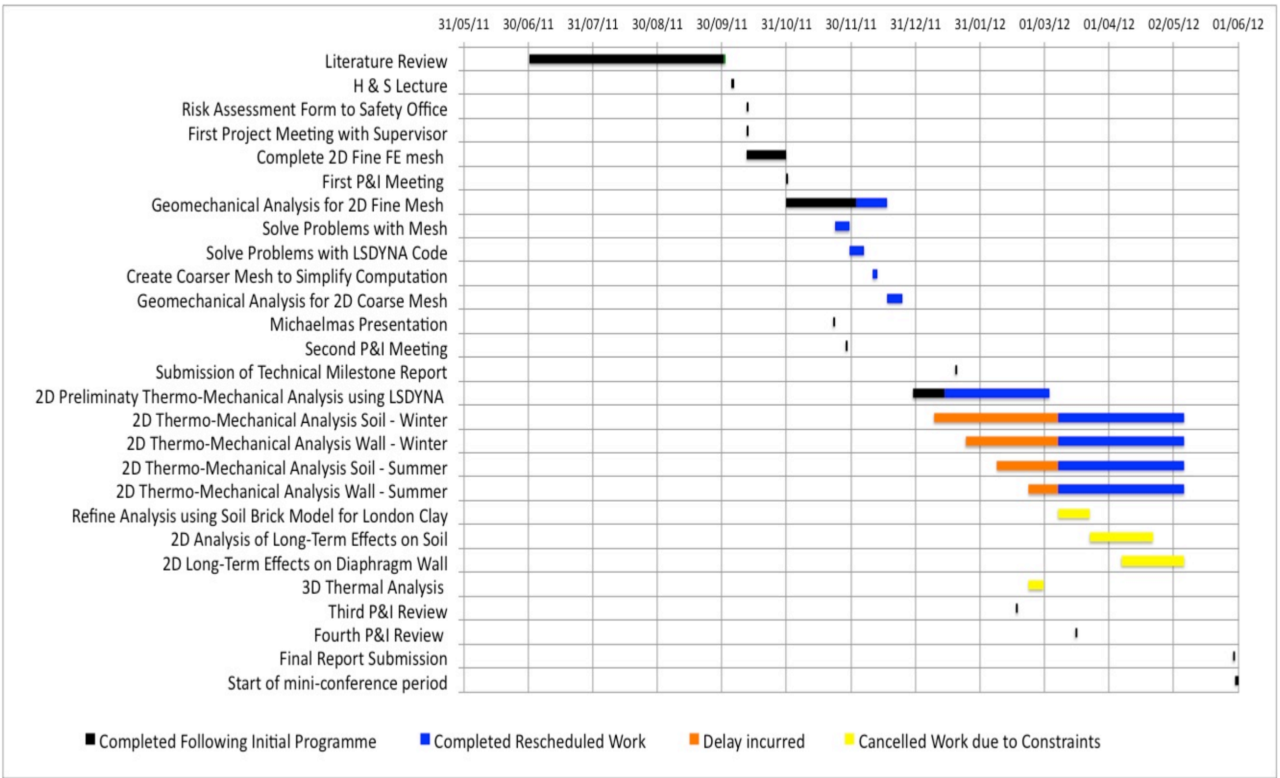

## References


[1] H. Brandl, (2006). "Energy foundations and other thermo-active ground structures". *Géotechnique,* 56, No. 2, 81-122.

[2] Lyesse Laloui, Mathieu Nuth and Laurent Vulliet, (2006). "Experimental and numerical investigations of the behaviour of a heat exchanger pile". *International Journal of Numerical and Analytical Methods in Geomechanics;* 30:763-781. Published online 15 February 2006 in Wiley InterScience (www.interscience.wiley.com). DOI: 10.1002/nag.499

[3] Wolfgang Unterberger, Hans Hofinger, Thomas Grünstäudl, Dietmar Adam & Roman Markiewicz, (2012). "Utilization of Tunnels as Sources of Ground Heat and Cooling – Practical Applications in Austria". *iC consulenten ZT GmbH, Salzburg, Austria & Dept. of Civil Engineering, Vienna University of Technology, Austria.* Published online 7 January 2012 in iC Group (http://www.ic-group.org/uploads/media/TunnelsGroundHeat_en.pdf). (16/5/2012).

[4] Tony Adams, (2011). "Energy Foundations in the UK". *Geothermal International Limited Business Development Director Presentation.* Published online in GSHPA (Ground Source Heat Pump Association) (http://www.gshp.org.uk/GroundSourceLive2011/TonyAmis_Piles_gsl.pdf). (16/5/2012).

[5] Fleur Loveridge, (2011). "Thermal behaviour of Piles as Heat Exchangers". *Ground Source Heat Pump Association Technical Seminar*, Cambridge.

[6] Kenichi Soga (2011). "Soil-structure interactions for thermal piles/walls; fundamentals; design considerations; future research needs". *Ground Source Heat Pump Association Technical Seminar*, Cambridge.

[7] GHC Bulletin, (2004). "Geotechnical (Ground-Source) Heat Pumps a World Overview". *Geo-Heat Centre, Oregon Institute of Technology, Klamath Falls, Oregon, USA. Institute of Applied Geosciences, Justus-Liebig University, Giessen, Germany. EarthEnergy Systems, GeoScience Ltd., Falmouth, Cornwall, UK. Department of Mathematical Physics, Lund University of Technology, Lund, Sweden.*

[8] Louis Lamarche, Stanislaw Kajl & Benoit Beauchamp, (2010). "A review of methods to evaluate borehole thermal resistances in geothermal heat-pump systems". École de Technologie Supérieure, Montréal. *Geothermics;* 39 (2010) 187-200. Published online 25 March 2010 in Elsevier (www.elsevier.com/locate/geothermics).

[9] Rosie Rawlings, (1999). "Ground Source Heat Pumps – A Technological Review". *A BSRIA Technical Note.* www.bsria.co.uk TN 18/1999.

[10] R.Curtis, J.Lund, B.Sanner, L.Rybach, G. Hellström, (2005). "Ground Source Heat Pumps – Geothermal Energy for Anyone, Anywhere: Current Worldwide Activity". *Proceedings World Geothermal Congress 2005, Antalya, Turkey. Geo-Heat Centre, Oregon Institute of Technology, Klamath Falls, Oregon, USA. Institute of Applied Geosciences, Justus-Liebig University, Giessen, Germany. EarthEnergy Systems, GeoScience Ltd., Falmouth, Cornwall, UK. Department of Mathematical Physics, Lund University of Technology, Lund, Sweden. Institute of Geophysics, ETH, Zurich and GEOWATT AG, Zurich, Germany.*

[11] Cementation Skanska. "Knightsbridge Palace Hotel. First UK use of geothermal loops in a diaphragm wall". *Online source.* http://www.skanska.co.uk/global/Sevices/Piling/Case%20Studies/Knightsbridge.pdf (16/5/2012).

[12] Tony Amis, Chris Robinson & Dr. Sam Wong, (2010) “Integrating geothermal loops into the diaphragm walls of the Knightsbridge Palace Hotel Project”. Basement and Underground Structures Conference. Geothermal International Ltd., Cementation Skanska Ltd., WSP Cantor Seinuk. *Online source.* (www.skanska.co.uk/global/Sevices/Piling/Case%20Studies/Knightsbridge.pdf) (16/5/2012).

[13] M.M. He & H.N. Lam, (2005). “Study of Geothermal Seasonal Cooling Storage System with Energy Piles”. *Mechanical Engineering Department, University of Hong Kong.*

[14] John A. Shonder & Patrick J. Hughes, (1998). “Increasing Confidence in Geothermal Heat Pump Design Methods”. *P.E. Oak Ridge National Laboratory.*

[15] Wei Yang, Jin Zhou, Wei Xu & Guoqiang Zhang, (2009). “Current Status of Ground-Source Heat Pumps in China”. *Energy Policy,* 38 (2010) 323-332. Published online 17 October 2009 in Elsevier (www.elsevier.com/locate/enpol).

[16] P. J. Bourne-Webb, B. Amatya, K. Soga, T. Amis, C.Davidson & P. Payne, (2009). “Energy Pile Test at Lambeth College, London: Geotechnical and Thermodynamic Aspects of Pile Response to Heat Cycles”. *Géotechnique,* 59, No. 3, 237-248, [doi: 10.1680/geot.2009.59.3.237].

[17] H. Brandl, (2009). “Energy Pile Concepts”. *Deep Foundations on Bored and Auger Piles - Van Impe & Van Impe (eds). 2009 Taylor Francis Group, London. ISBN 978-0-415-47556-3.*

[18] Katzenbach, R., Ramm, H. & Waberseck, T., (2009). “Recent Developments in Foundation and Geothermal Engineering”. *2nd International Conference on New Developments in Soil Mechanics and Geotechnical Engineering. 28-30 May 2009, Near East University, Nicosia, North Cyprus. (Technische Universität Darmstadt, Institute of Geotechnics, Germany).*

[19] Energy Saving Trust, (2007). “Domestic Ground Source Heat Pumps: Design and installation of closed-loop systems. A guide for specifiers, their advisors and potential users”. *Energy Saving Trust, CE82, London.*

[20] Kevin Rafferty, (1997). “An Information Survival Kit for the Prospective Residential Geothermal Heat Pump Owner”. *GHC Bulletin, April 1997. Geo-Heat Centre.*

[21] Yi Rui, (2011). “Finite Element Modelling of Geothermal Problems”. *1st. Year PhD Report. Department of Engineering, University of Cambridge.*

[22] A. Di Domenico & C. Davidson, (2011). “Ground Source Heat Pump System. Design Statement. Tottenham Court Road, Dean Street”. *Geothermal International & Crossrail.*

[23] Richard Sturt, (2011). “Dean Street: Geothermal wall: Thermal analysis”. *Arup Presentation by Richard Sturt, 11th March 2011.*

[24] L.Wong, A. Pillai, D. Harris & R. Main, (2011). “Analysis Report for 3D FE Model of Tottenham Court Road Station West Box”. *Crossrail Design Consultant Framework Contract C122 – Bored Tunnels.*

[25] A.Pillai, R. Sturt & D. Nicholson, (2011). “Tottenham Court Road – Dean Street Station. Geothermal Wall: Preliminary Thermal Analysis of Heat Extraction”. *Crossrail & Arup Documentation.*

[26] Duncan Nicholson, (2011). “Assessing the latest advances in thermal piling”. *Piling and Foundations UK, 10th May 2011. Arup.*

[27] Livermore Software Technology Corporation (LSTC), (2009). “LS-DYNA ® Keyword User’s Manual – Volume 1”. *June 2009, Version 971/Release 4, Beta.*

[28] FWT Ltd. Online source for seasonal temperature fluctuations in soil. Image published online at http://www.filterclean.co.uk/images/info1geothermal/ground_hp_chart_opt.jpg. (16/5/2012).

[29] Jonathan Busby, BGS (British Geological Survey) (2011). "Provision of thermal properties". *Ground Source Heat Pump Association (GSHPA) Technical Seminar, Cambridge. 2011.*

[30] Flickr. Dean Street Station Site Photograph prior to over-site building construction. Online resource: http://www.flickr.com/photos/kpmarek/4181640270/in/photostream/. (18/5/2012)

[31] The Green Age web resource. *Ground Source Heat Pumps.* Online resource: http://www.thegreenage.co.uk/ghome/ground-source-heat-pumps (18/5/2012)

[32] Mark A. Christon & Grant O. COOK JR, (2001). "LS-DYNA's Incompressible Flow Solver User's Manual". *Livermore Software Technology Corporation. Version 960, Development Version, March 2001.* (http://ftp.lstc.com/anonymous/outgoing/trent001/manuals/old/ls-dyna_incompfluid_manual.pdf), (18/5/2012).

[33] A.W. Al-Kayssi, A. A. Al-Karaghouli, A. M. Hasson & S. A. Becker, (2005). "Influence of soil moisture content on soil temperature and heat storage under greenhouse conditions". *Journal of Agricultural Engineering Research.* Vol.45, 241-252. Publishe online 8 September 2005 at Elsevier, http://www.sciencedirect.com/science/article/pii/S0021863405801520. (19/5/2012).

[34] Z. Q. Chen & M. H. Shi, (2004). "Study of heat and moisture migration in porous building materials". *Applied Thermal Engineering.* Vol. 25, Issue 1, 61-71. Published online 13 August 2004 at Elsevier, http://www.sciencedirect.com/science/article/pii/S1359431104001164. (19/5/2012).

[35] International Energy Agency, (2011). "Technology Roadmap. Energy-efficient buildings: Heating and Cooling Equipment". *International Energy Agency.* Online source: http://www.iea.org/papers/2011/buildings_roadmap.pdf. (21/5/2012).

[36] University of West England. "Basic Mechanics of Soils". *University of West England, Bristol.* Online source: http://environment.uwe.ac.uk/geocal/SoilMech/basic/soilbasi.htm. (21/5/2012)